ELSEVIER

Morphological colour operators in totally ordered lattices based on distances: Application to image filtering, enhancement and analysis

Jesús Angulo *

Centre de Morphologie Mathématique—Ecole des Mines de Paris, 35, rue Saint-Honor, 77305 Fontainebleau, France

Abstract

The extension of mathematical morphology operators to multi-valued functions, and in particular to colour images, is neither direct nor general. In this paper, a generalisation of distance-based and lexicographical-based approaches is proposed, allowing the extension of morphological operators to colour images for any colour representation (e.g., RGB, LSH and L*a*b*) and for any metric distance to a reference colour. The performance of the introduced operators is illustrated by means of different applications: colour feature extraction using openings (closings) by reconstruction, colour gradients for segmenting, colour denoising by the centre operator and colour enhancement by the contrast mapping. Examples from natural colour images and biomedical microscopic colour images are given.
© 2007 Elsevier Inc. All rights reserved.

1. Introduction

Mathematical morphology is the application of lattice theory to spatial structures. This means that the definition of morphological operators needs a totally ordered complete lattice structure, i.e., the possibility of defining an ordering relationship between the points to be processed. Therefore, the application of mathematical morphology to colour images is difficult due to the vectorial nature of the colour data. For a general account on mathematical morphology the interested reader should refer to [44,21], whereas vector morphology is extensively discussed in [46,17,50].

Multivariate data ordering is not straightforward, because there is no notion of natural ordering in a vector field, as opposed to one-dimensional (scalar) case [8]. To overcome the problem, the following four approaches to ordering multichannel samples, such as colour data, have been identified [8,40,31]. In *marginal ordering* (M-ordering) the components of the colour vectors are ordered independently (pointwise ordering). However, this approach produces new colour vectors which were not originally present in the input image, thus often introducing colour artifacts into the output image [46]. To preserve the input colour vectors, the *conditional ordering* (C-ordering) approach, also known as lexicographic ordering, is frequently used. The C-ordering produces the ordered set of the colour vectors according to the ordering of one component or more generally, some marginal components selected sequentially according to different conditions. When all the components are used, the C-ordering is a total ordering. Note that this approach does not use the full vectorial nature of the input. The *partial ordering* or P-ordering is based on the partition of the vectors into groups, such that the groups can be distinguished with respect to rank or extremeness. This is computed by using convex-hull like

* Fax: +33 1 64 69 47 07.
  E-mail address: jesus.angulo@ensmp.fr
  URL: http://cmm.ensmp.fr/~angulo

sets. The *reduced ordering* or R-ordering which performs the ordering of vectors according to some scalars, computed from the components of each vector with respect to different measure criteria, typically distances or projections onto a reduced space (using for instance the principal component analysis). The application of P- or R-orderings also preserves the input colour vectors.

As discussed in the sequel, the above ordering approaches have been used to support morphological operations on colour data. For example, in [46], Serra suggested an intermediate ordering between an M-ordering and a C-ordering. Weber and Acton [54] introduced an M-ordering in HSV colour space by using a rotation in the hue band (shifting the *H* discontinuity by *k*-means clustering).

The C-ordering has been also widely studied in the framework of colour morphology, especially in a luminance/saturation/hue representation, by Peters [39], by Talbot et al. [50], by Hanbury and Serra [18], by Ortiz et al. [37], by Louverdis et al. [28], and by Angulo [5]. The C-ordering has been also applied in the RGB representation by Iwanowski and Serra [23], and by Angulo and Serra [4]; or in the Lab representation by Hanbury and Serra [20]. Vardavoulia et al. [52] defined also vectorial median filters with C-orderings.

A P-ordering is the starting point, in a fuzzy logic paradigm, for a method proposed by Köppen et al. [25] to implement Pareto fuzzy colour morphology. Another P-ordering has been introduced by Mojsilovic and Soljanin [35], using a sampling based on the Fibonacci succession. Gibson et al. [16] used a local convex hull to define the pixels of a region as extreme/non-extreme, which is necessary to build morphological connected operators.

The R-ordering has been widely used in colour denoising applications (i.e., vector median filters and other statistical filters) by Astola et al. [7], by Pitas and Tsakalides [40], by Trahanias et al. [51], and more recently by Lukac et al. [31,32]. The R-ordering has been also used to build morphological operators by means of Euclidean distances by Comer and Delp [15] and by Ortiz et al. [36]; or using Mahalanobis distances by Goutsias et al. [17], and by Al-Otum [1]. Sartor and Weeks [55,43] proposed a combination of an R-ordering and a C-ordering; in fact, our present approach can be considered as a generalisation of this interesting study. In [27], J. Li and Y. Li proposed an R-ordering based on fuzzy first principal component in RGB colour space, and in [56], Wheeler and Zmuda a R-ordering with vector projections in RGB. And in [59], Zaharescu et al. explored R-orderings based on a geometrical interpretation of a triangle representation of colours.

Other alternative total orderings have been studied. Goutsias et al. [17] used the matrix Wilson theory [57]. Chanussot and Lambert [14] suggested an approach based on space-filling curves. In [12], Busch and Eberle proposed a pseudo-morphology for colour-coded (or labeled) images by introducing the ordering according semantic rules (a C-ordering). It is also possible to define an ordering on labels, such as the hue component image, by adding a bottom element (meaning no hue) and a top element (meaning hue conflict), see details in the work of Ronse and Agnus [42].

The aim of this paper is to generalise the distance-based approaches and the lexicographical approaches, in order to propose a generic framework allowing the extension of morphological operators to colour images for any colour representation and metric distance. The proposed approach is a combination of R-ordering and C-ordering, the R-ordering being based on the distance to a reference colour and a subsequent lexicographical ordering used to resolve any ambiguities. In fact, we introduce a generalisation of mathematical morphology to multivariate functions, according to a distance-to-origin-based interpretation of the notion of total ordering between the points of a complete lattice. Whilst the use of a combination of suborderings to produce a total ordering is not new, the approach presented here does have some distinctive features, in particular its applicability to different colour spaces/distances and the use of any reference colour (including colours other than black and white).

The rest of the paper is organised as follows. In Section 2 we give a reminder on some notions of colour representation and colour distances. In Section 3, a discussion of our framework of total orderings using distances completed with lexicographical cascades is given. Then, in Section 4, we introduce the definition on the derived main morphological colour operators. The performances of these transformations for filtering, noise reduction, enhancement and feature extraction are illustrated in Section 5. Finally, the conclusions and perspectives are discussed in Section 6.

2. Colour representations and colour distances

The most direct way to manipulate digital colour images is to work on the RGB colour space. However, the RGB colour representation has some drawbacks: strongly correlated components, lack of human interpretation, non-uniformity, etc. A polar representation with the variables luminance, saturation and hue (lum/sat/hue) allows us to solve these problems. The HLS system is the most popular lum/sat/hue triplet. In spite of its popularity, the HLS representation (and another classical one like HSV) often yields unsatisfactory results, for quantitative processing at least, because its luminance and saturation expressions are not norms, so average values or distances, are falsified. The drawbacks of the HLS system can be overcome by various alternative representations, according to different norms used to define the luminance and the saturation. The reader can find a comprehensive analysis of this question by Angulo and Serra [6]. In particular, we have used in this paper the lum/sat/hue in norm L_1 [47,48,6]. In the present study, we have also worked with the $L^*a^*b^*$ colour space, the classical representation in colorimetry, which presents a perceptual uniformity (useful for segmentation). The transformations between RGB and $L^*a^*b^*$ are well-known [24,58].

Let f be a grey-level image, $f : E \rightarrow \mathscr{T}$, in that case $\mathscr{T} = \{t_{\min}, t_{\min} + 1, \cdots, t_{\max}\}$ (in general $\mathscr{T} \subset \mathbb{Z}$ or $\mathbb{R}$) is

an ordered set of grey-levels and typically for the digital 2D images $E \subset \mathbb{Z}^2$ is the support of the image. We denote by $\mathcal{F}(E, \mathcal{T})$ the functions from E onto $\mathcal{T}$. If $\mathcal{T}$ is a complete lattice, then $\mathcal{F}(E, \mathcal{T})$ is a complete lattice too. The theoretical framework of mathematical morphology is nowadays phrased in terms of complete lattices and operators defined on them. Given the three sets of scalar values $\mathcal{T}^l, \mathcal{T}^s, \mathcal{T}^h$, we denote by $\mathcal{F}(E, [\mathcal{T}^l \otimes \mathcal{T}^s \otimes \mathcal{T}^h])$ or $\mathcal{F}(E, \mathcal{T}^{lsh})$ all colour images in a luminance/saturation/hue representation ($\mathcal{T}^{lsh}$ is the product of $\mathcal{T}^l, \mathcal{T}^s, \mathcal{T}^h$, i.e., $\mathbf{c}_i \in \mathcal{T}^{lsh} \Longleftrightarrow \mathbf{c}_i = \{(l_i, s_i, h_i); l_i \in \mathcal{T}^l, s_i \in \mathcal{T}^s, h_i \in \mathcal{T}^h\}$). We denote the elements of $\mathcal{F}(E, \mathcal{T}^{lsh})$ by $\mathbf{f}$, where $\mathbf{f} = (f_L, f_S, f_H)$ are the colour component functions. Using this representation, the value of $\mathbf{f}$ at a point $x \in E$, which lies in $\mathcal{T}^{lsh}$, is denoted by $\mathbf{f}(x) = (f_L(x), f_S(x), f_H(x))$. In a similar way, the colour images in a RGB representation or in a L*a*b representation are respectively elements of the product sets $\mathcal{F}(E, \mathcal{T}^{rgb})$ and $\mathcal{F}(E, \mathcal{T}^{L^*a^*b^*})$. Note that the sets $\mathcal{T}^r, \mathcal{T}^g, \mathcal{T}^b$ are complete totally ordered lattices. The sets $\mathcal{T}^l, \mathcal{T}^s$ corresponding to the luminance and the saturation are also totally ordered lattices (likewise the components of L*a*b* $\mathcal{T}^{L^*}, \mathcal{T}^{a^*}$ and $\mathcal{T}^{b^*}$). The hue component is an angular function defined on the unit circle, $\mathcal{T}^h = \mathscr{C}$, which has no partial ordering. Hence, the hue needs to be processed in a special way. Let $h : E \to \mathscr{C}$ be an angular function, the angular difference [39,19] is defined as

$$h_i \div h_j = \begin{cases} |h_i - h_j| & \text{if} \quad |h_i - h_j| \leqslant 180° \\ 360° - |h_i - h_j| & \text{if} \quad |h_i - h_j| > 180° \end{cases} \quad (1)$$

Therefore, it is possible to fix an origin on the hues denoted by h_0, associated to a "colour of reference". We can now define a h_0-centered hue function by computing $f_H(x) \div h_0$. The function $(f_H \div h_0)(x)$ is a partially ordered set (i.e., two hue values can have the same angular distance to the origin). In order to have a total order we need to impose an additional priority (absolute distance to the origin h_0 in the sense of the unit circle), see [2]. This totally ordered complete lattice is denoted by $\mathcal{T}^{h \div h_0}$.

Let $\mathbf{c}_k = (c_k^U, c_k^V, c_k^W)$ be the colour point k in any generic colour space UVW (e.g., in LSH $\mathbf{c}_k = (c_k^L, c_k^S, c_k^H)$). We can now define the colour distance between two colour vectors i and j as $||\mathbf{c}_i - \mathbf{c}_j||_\Delta^{UVW}$ where Δ is a particular metric.

The family of Minkowski metric distances $d_L(\mathbf{c}_i, \mathbf{c}_j) = (\sum_{n=1}^3 |c_i^n - c_j^n|^L)^{1/L} = ||\mathbf{c}_i - \mathbf{c}_j||_L$, is the most commonly used measure to quantify colour distances. The most popular members of this class of metrics are obtained when $L = 1$ (city-block distance), $L = 2$ (Euclidean distance) and $L = \infty$ (chessboard distance). The Mahalanobis distance is a special case of the quadratic-form generalised distance metric in which the transform matrix is given by the covariance matrix Γ obtained from a training set of data that represents the reliability or scale of the measurement in each direction. The Mahalanobis distance between two vectors is given by $||\mathbf{c}_i - \mathbf{c}_j||_M = (\mathbf{c}_i - \mathbf{c}_j)^T \Gamma^{-1} (\mathbf{c}_i - \mathbf{c}_j)$.

Any of the above recalled metrics can be applied to colour vectors according to the different colour space representations, e.g., in RGB using L_2 we have $||\mathbf{c}_i - \mathbf{c}_j||_2^{RGB} = \sqrt{(c_i^R - c_j^R)^2 + (c_i^G - c_j^G)^2 + (c_i^B - c_j^B)^2}$. The L_2 distance in L*a*b* is particularly used in image processing, indeed the perceptual difference between two colours in L*a*b* is given by their Euclidean distance. Other more sophisticated colour distances have been proposed in the literature [31]. From the mathematical morphology point of view, some issues must be taken into account. As pointed out above, the functions associated with the RGB components, with the L*a*b* components (although the ordering for chromatic components a* and b* is hardly meaningful), and with the luminance and saturation components of the LSH representation are complete totally ordered lattices, but not the hue. Therefore, for all the colour metric distances in LSH, the term associ-ated to the hue must use the angular difference, e.g., $||\mathbf{c}_i - \mathbf{c}_j||_1^{LSH} = |c_i^L - c_j^L| + |c_i^S - c_j^S| + |c_i^H \div c_j^H|$.

Nevertheless, due to the instability of the hue component for the low saturation points (which is an important issue to build hue-based distances, gradients, ordering, etc.) this last distance is useless. In order to cope with this drawback, the different solutions are generally based on a weighting of the hue by the saturation [13,18,5]. We propose to use the simplest technique, multiplying the angular difference by the average saturation, i.e., $\frac{(c_i^S + c_j^S)}{2} |c_i^H \div c_j^H|$. As suggested in [13], other more sophisticated saturation-based weighing functions can be applied (e.g., sigmoid). Another more interesting way to compute colour distances in LSH representation involves working in polar coordinates, i.e., $||\mathbf{c}_i - \mathbf{c}_j||_2^{LSH} = \sqrt{(c_i^L - c_j^L)^2 + (c_i^S)^2 + (c_j^S)^2 - 2c_i^S c_j^S \cos(c_i^H \div c_j^H)}$. We suggest to use this last colour distance.

Before applying these colour distances to define morphological operators, a relevant analysis of the alternative distances shall be made. Firstly, the L_∞ norm distances could cause serious artefacts in the filtered colour images, since colour vectors will be ordered according to only one of the components, which can change for a set of points. We can suppose that the results according to L_1 or L_2 will be relatively similar. In fact, the Mahalanobis distance can be interpreted as their generalisation with the advantage of setting different weights for the components. Moreover, for the sake of simplicity of this paper, we consider that in the three colour representations the components are statistically independent and we can rewrite the Mahalanobis distance as a weighting distance, i.e., $||\mathbf{c}_i - \mathbf{c}_j||_{M(\omega_1, \omega_2, \omega_3)}^{UVW} = \omega_1(c_i^U - c_j^U)^2 + \omega_2(c_i^V - c_j^V)^2 + \omega_3 (c_i^W - c_j^W)^2$.

3. Colour total orderings using distances completed with lexicographical cascades

We have previously studied in depth the extension of morphological operators to colour images based on lexicographical cascades from a LSH representation [2,5]. Fig. 1
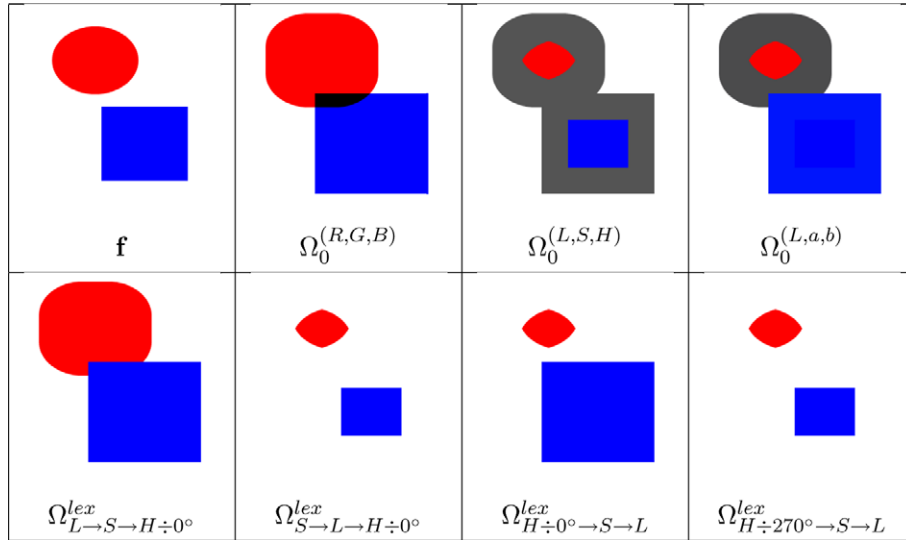
Fig. 1. Comparison of colour erosion for the image $\mathbf{f}$ (the structuring element B is a square of size $n = 35$), $\varepsilon_{\Omega, nB}(f)$, using different orderings Ω: three examples of marginal orderings Ω_0 in the RGB, LSH and $L^*a^*b^*$ colour spaces and four examples of total lexicographic-based orderings Ω^{lex} in LSH giving the priority to the luminance, or to the saturation, or to the h_0-centred hue (origins in the red 0° and in the purple 270°). (For interpretation of the references to color in this figure legend, the reader is referred to the Web version of this article.)

shows a comparison of colour erosion for the image $\mathbf{f}$, using different orderings Ω. Namely, three examples of marginal orderings Ω_0 in the RGB, LSH and $L^*a^*b^*$ colour spaces and four examples of total lexicographic-based orderings Ω^{lex}. We observe the appearance of false colours when the marginal processing is applied, i.e., starting from two colours, the erosion gives another one; moreover the interpretation of results in LSH or $L^*a^*b^*$ becomes tricky. The original colours are preserved when the lexicographical cascades in LSH are used. In addition, giving the priority to the luminance (the background—brightest colour—is eroded), or to the saturation (the most saturated colours are eroded), or to the h_0-centred hue (origins in the red 0° and in the purple 270°), we can act on the structures mainly by the first component chosen in the cascade. The rationale behind the approach developed in this paper is more ambitious, proposing a generic framework valid for any colour representation and adding the flexibility of a "reference colour"-based morphology.

3.1. Distance-based grey-level morphology

The effect of morphological operators is determined by the specification of a partial ordering on the underlying image space, or from an image processing viewpoint, by the choice of what is foreground and what is background [22]. Usually, in grey-level images, the foreground corresponds to the bright levels (close to $t_{\max}$) and the background to the dark ones (close to $t_{\min}$). The associated partial ordering is the usual ordering $\leqslant$, which can be used to compute the infimun $\wedge$ and the supremum $\vee$ between a set of pixels B (structuring element). Then, the two basic morphological operators erosion and dilation applied to a grey-level image $f(x)$ are given by: $\varepsilon_B(f(x)) = \{f(y):$

$f(y) = \wedge[f(z)], \ z \in B_x\}$ and $\delta_B(f(x)) = \{f(y):f(y) = \vee[f(z)], z \in B_x\}$, respectively.

After defining as reference the maximum grey value $g_0 = t_{\max}$, the classical greyscale morphology can be also interpreted in terms of distance to this reference:

- the dilation δ tends to move toward this reference, i.e., δ at point x is the grey value which has minimal distance to the reference g_0 within the structuring element B centered at x:

$$\delta_B(f(x)) = \{f(y) : y = \arg_z \inf(|f(z) - t_{\max}|), z \in B_x\}, \quad (2)$$

- the erosion ε tends to move away from g_0; i.e., ε is the value with maximal distance to g_0,

$$\varepsilon_B(f(x)) = \{f(y) : y = \arg_z \sup(|f(z) - t_{\max}|), z \in B_x\}. \quad (3)$$

In fact, this is only the convention that we have adopted. It is also possible to define the dilation (erosion) as the operation which tends to move away from (toward) the reference g_0, but the reference being the minimum grey value $g_0 = t_{\min}$. In this case, the dilation is given by

$$\delta_B(f(x)) = \{f(y) : y = \arg_z \sup(|f(z) - t_{\min}|), z \in B_x\},$$

and the dual expression defines the erosion.

Fig. 2 depicts an example of grey-level dilation and erosion in terms of distance to a reference value (R-ordering), when this reference is $t_{\max}$. We note the need of a reference value to fix a partial ordering. Actually, we can define two operators based on the distance between the grey-levels but which are independent from the reference. To do that, the cumulative distance of each point to the other points within the structuring element, i.e., $D(f(x)) = \sum_k d_E(f(x), f(k))$, $k \in B_x$, is firstly calculated. Then, the *distance-based median*
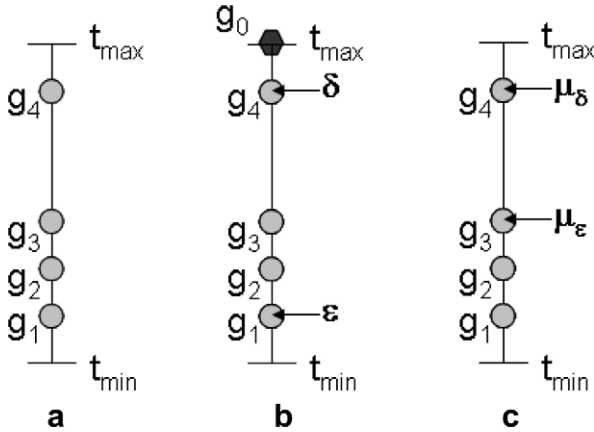
Fig. 2. Example of grey-level dilation and erosion in terms of distance to the reference value (R-ordering): (a) four original scalar points, $g_i \in \mathcal{T}$, to be processed, (b) corresponding values of dilation δ and erosion ε when the reference is $g_0 = t_{\max}$. In (c) are given the values of the median μ_ε and the anti-median μ_δ defined in terms of the cumulative distance.

is defined as $\mu_\varepsilon(f(x)) = \{f(y): y = \arg_z \inf(D(f(z)),\ z \in B_x\}$; and by duality, the *distance-based anti-median* is defined as $\mu_\delta(f(x)) = \{f(y): y = \arg_z \sup(D(f(z)),\ z \in B_x\}$. Fig. 2 gives also the corresponding example of this "eccentricity"-based operators. A classical generalisation of these definitions to multi-channel images leads to the vector median filters [7,40]. Several works, see for instance Plaza et al. [41], propose to use these two filters to define multispectral morphological operators, however, it is easy to see that the obtained operators are not an adjunction erosion/dilation. In particular, μ_ε and μ_δ do not commute with the infimum and supremum, respectively, a property underlying the definition of erosion and dilation. At the most, we can consider μ_ε and μ_δ as pseudo-morphological operators. We believe that any generalisation of morphological operators to multivariate functions (e.g., colour images) must be compatible with the definitions of these operators for univariate functions (grey-level images).

3.2. Total orderings associated with a reference colour

The paradigm of distance-to-reference-based grey morphology is directly applicable to colour images, after fixing the colour representation UVW, the reference colour $\mathbf{c}_0$ and the colour distance $\varDelta$, by defining the following ordering for two colour points:

$$\mathbf{c}_i <_{\mathbf{c}_0} \mathbf{c}_j \iff \|\mathbf{c}_i - \mathbf{c}_0\|_{\varDelta}^{\mathrm{UVW}} > \|\mathbf{c}_j - \mathbf{c}_0\|_{\varDelta}^{\mathrm{UVW}}. \tag{4}$$

But this is only a partial ordering or pre-ordering, i.e., two or more distinct colour vectors within the structuring element can be equidistant from the reference. This problem also arises in the grey-level case if the erosion and dilation are defined by the distance to a reference g_0 which is different from the bounds $t_{\max}$ or $t_{\min}$. For example, fixing $t_{\max} = 255$, $t_{\min} = 0$ and $g_0 = 100$, given two grey pixels $g_1 = 50$ and $g_2 = 150$, one has $|g_1 - g_0| = |g_2 - g_0|$ with $g_1 \neq g_2$ and consequently, the supremum/infimum between

both pixels are not defined. An additional condition is needed to complete the ordering; for instance, fixing the following ordering: $g_i <_{g_0} g_j \iff (|g_i - g_0| > |g_j - g_0|)$ or $(|g_i - g_0| = |g_j - g_0|$ and $g_i > g_j)$. For the previous example, it is obtained that $g_1 = 50 >_{g_0} g_2 = 150$. More specifically, in order to have a total ordering for colour images we propose to complete the primary R-ordering of relation (4) with a lexicographical cascade.

The total Ω-ordering or $<_\Omega$ is defined as:

$$\mathbf{c}_i <_\Omega \mathbf{c}_j \iff \begin{cases} \|\mathbf{c}_i - \mathbf{c}_0\|_{\varDelta}^{\mathrm{UVW}} > \|\mathbf{c}_j - \mathbf{c}_0\|_{\varDelta}^{\mathrm{UVW}} \quad \text{or} \\[4pt] \|\mathbf{c}_i - \mathbf{c}_0\|_{\varDelta}^{\mathrm{UVW}} = \|\mathbf{c}_j - \mathbf{c}_0\|_{\varDelta}^{\mathrm{UVW}} \quad \text{and} \\[4pt] \begin{cases} c_i^U < c_j^U \quad \text{or} \\[4pt] c_i^U = c_j^U \quad \text{and} \quad c_i^V < c_j^V \quad \text{or} \\[4pt] c_i^U = c_j^U \quad \text{and} \quad c_i^V = c_j^V \quad \text{and} \quad c_i^W < c_j^W \end{cases} \end{cases} \tag{5}$$

We denote, compactly, this lexicographical cascade by $\Omega \equiv \{\|\cdot\|_{\varDelta}^{\mathrm{UVW}}, \mathbf{c}_0 = (c_0^U, c_0^V, c_0^W) \vdash (U \to V \to W)\}$. Moreover, in the examples given below, when the Mahalanobis distance $\|\cdot\|_{M(\omega_1,\omega_2,\omega_3)}^{\mathrm{UVW}}$ is applied, the component k of the reference colour $\mathbf{c}_0$ can be undefined (or unsignificant), which is denoted by "–", if the weight k is zero $\omega_k = 0$; e.g., $\|\cdot\|_{M(0,1,2)}^{\mathrm{UVW}}$, $\mathbf{c}_0 = (-, 255, 128)$.

In the ordering (5), after a comparison based on the $\varDelta$ distance to c_0, the priority is given to the component U, then to V and finally to W. Obviously, it is possible to define other orders for imposing a dominant role to any other of the vector components. To simplify the number of alternatives, and based on the best results obtained from our previous works on lexicographical cascades, we propose to fix the ordering of the components for the three colour spaces representations as follows,

(1) in RGB: $\vdash (G \to R \to B)$,
(2) in LSH: $\vdash (L \to S \to -(H \div h_0))$, where the origin of the hues h_0 corresponds to the same as for $\mathbf{c}_0^{\mathrm{LSH}} = (l_0, s_0, h_0)$; and $h_i \div h_0$ is obtained by means of Eq. (1),
(3) in L*a*b*: $\vdash (L \to a \to b)$.

Note that one easily verifies that the family of colour orderings given by the expression (5) generalises the lexicographical orderings, i.e., using the weighing distance $\|\cdot\|_M^{\mathrm{UVW}}$ with the weights $M(\omega_1, \omega_2, \omega_3) = M(1,0,0)$ and the reference equals to the upper bound of axis U, $\mathbf{c}_0 = (c_{\max}^U, -, -)$, the relation (5) is equivalent to the ordering $\Omega_{U \to V \to W}^{\mathrm{lex}}$:

$$\mathbf{c}_i <_{\Omega^{\mathrm{lex}}} \mathbf{c}_j \iff \begin{cases} c_i^U < c_j^U \quad \text{or} \\[4pt] c_i^U = c_j^U \quad \text{and} \quad c_i^V < c_j^V \quad \text{or} \\[4pt] c_i^U = c_j^U \quad \text{and} \quad c_i^V = c_j^V \quad \text{and} \quad c_i^W < c_j^W \end{cases}$$

3.3. Erosion and dilation on complete lattice $\mathcal{T}^{uvw}$

Using the total Ω-ordering $<_\Omega$ we have $\mathbf{c}_i = \mathbf{c}_j$ or $\mathbf{c}_i <_\Omega \mathbf{c}_j$ or $\mathbf{c}_j <_\Omega \mathbf{c}_i$ for every pair $(\mathbf{c}_i, \mathbf{c}_j)$. Therefore, it is defined for any family of colour points $(\mathbf{c}_k)_{k \in I} \in \mathcal{T}^{uvw}$ the colour supremum $\sup_\Omega[\mathbf{c}_k] = \bigvee_{k \in I}^{\mathbf{c}_0} \mathbf{c}_k$ and the colour infimum $\inf_\Omega[\mathbf{c}_k] = \bigwedge_{k \in I}^{\mathbf{c}_0} \mathbf{c}_k$. Furthermore, the following extremes exist for the complete lattice $\mathcal{T}^{uvw}$: the upper bound ("greatest colour") is $\mathbf{c}_0$ itself, i.e., $\top^{\mathbf{c}_0} = \mathbf{c}_0$; the lower bound ("smallest colour"), $\perp_{\mathbf{c}_0}$, is the most distant colour point of $\mathbf{c}_0$. In fact, $\perp_{\mathbf{c}_0}$ corresponds to one of the extremal points of bounded space $\mathcal{T}^u \times \mathcal{T}^v \times \mathcal{T}^w$; e.g., in RGB (each grey-level component $\in [0,255]$) with $\mathbf{c}_0 = (10,10,200)$ the lower bound is the corner of the RGB cube $\perp = (255,255,0)$.

The theory of adjunctions on complete lattices has played an important role in mathematical morphology [44,21]. In particular, using the major results, the most general definition of erosion and dilation is as follows. The operator ε between the complete lattice $\mathcal{T}^{uvw}$ and itself is an erosion if $\varepsilon(\bigwedge_{k \in I}^{\mathbf{c}_0} \mathbf{c}_k) = \bigwedge_{k \in I}^{\mathbf{c}_0} \varepsilon(\mathbf{c}_k)$ for every family $(\mathbf{c}_k)_{k \in I}$. A similar dual definition holds for dilation δ (i.e., commutation with the supremum). The pair (ε, δ) is called an adjunction between $\mathcal{T}^{uvw} \to \mathcal{T}^{uvw}$ if $\delta(\mathbf{c}_y) \leqslant_\Omega \mathbf{c}_x \Longleftrightarrow \mathbf{c}_y \leqslant_\Omega \varepsilon(\mathbf{c}_x)$. Moreover, to every erosion ε corresponds a unique dilation δ given by $\delta(\mathbf{c}_y) = \bigwedge^{\mathbf{c}_0} \{\mathbf{c}_x \in \mathcal{T}^{uvw} : \mathbf{c}_y \leqslant_\Omega \varepsilon(\mathbf{c}_x)\}$ such that (ε, δ) is an adjunction. These theoretical definitions are interesting to consider if the proposed colour ordering verifies the basic properties of erosion/dilation, however, they do not allow computing erosion/dilation in practice. We recall the algorithmic definition of colour erosion and dilation, and derived operators, in the next section.

3.4. Complementary colours and quasi-duality

One of the most interesting properties of (binary and grey-level) morphological operators is the duality by the complementation. Let $f(x) \in \mathscr{F}(E, \mathcal{T})$ be a grey-level image, where $\mathcal{T}$ is bounded by $[t_{min}, t_{max}]$. The complement image (or negative image) $\overline{f}(x)$ is defined as the reflection of $f(x)$ with respect to $(t_{min} + t_{max})/2$; i.e., $\overline{f}(x) = t_{max} - f(x) + t_{min}$, $\forall x \in E$. Let the pair $(\varepsilon, \delta) : \mathscr{F}(E, \mathcal{T}) \to \mathscr{F}(E, \mathcal{T})$ be an adjunction, that is let $\varepsilon(f)$ and $\delta(f)$ be respectively an erosion and its associated dilation in $\mathscr{F}(E, \mathcal{T})$. The property of duality holds:

$$\varepsilon(\overline{f}) = \overline{\delta(f)} \Rightarrow \varepsilon(f) = \overline{\delta(\overline{f})},$$

and this is verified for any other pair of dual operators, such as the opening/closing. In practice, this property allows us to implement exclusively the dilation, and using the complement, to be able to obtain the corresponding erosion.

The complement of a colour image, $\mathbf{f} \in \mathscr{F}(E, \mathcal{T}^{uvw})$, is defined as the complement of each colour component; i.e., $\overline{\mathbf{f}} = (\overline{f}_U, \overline{f}_V, \overline{f}_W)$. Moreover for each colour pixel i the complementary colour is given by $\overline{\mathbf{c}}_i = (c_{max}^U - c_i^U + c_{min}^U, c_{max}^V - c_i^V + c_{min}^V, c_{max}^W - c_i^W + c_{min}^W)$, where c_{max}^U and c_{min}^U are, respectively, the upper and lower bounds of $\mathcal{T}^u$ (idem. for V and W components). We need to study if there exists an equivalent property of duality for colour operators according to the family of orderings given by (5). Let us use for our discussion the example of Fig. 3. For the sake of simplicity, it deals with a two dimensional case: the bounded vector space $[x_{min}, x_{max}] \times [y_{min}, y_{max}]$. The simplified total ordering is

$$\mathbf{v}_i <_{\mathbf{v}_0} \mathbf{v}_j \Longleftrightarrow \begin{cases} \|\mathbf{v}_i - \mathbf{v}_0\|_2 > \|\mathbf{v}_j - \mathbf{v}_0\|_2 & \text{or} \\ \|\mathbf{v}_i - \mathbf{v}_0\|_2 = \|\mathbf{v}_j - \mathbf{v}_0\|_2 & \text{and} \begin{cases} x_i < x_j & \text{or} \\ x_i = x_j & \text{and} \quad y_i < y_j \end{cases} \end{cases}$$

Let $(\mathbf{v}_i)_{i \in I}$ be a family of nine points and $\mathbf{v}_0$, $\mathbf{v}_0'$, $\mathbf{v}_0''$ and $\mathbf{v}_0'''$ be four reference points. Choosing the reference $\mathbf{v}_0$ in Fig. 3(a), we obtain the supremum $\bigvee_{i \in I}^{\mathbf{v}_0} \mathbf{v}_i = \mathbf{v}_3$ and the infimum $\bigwedge_{i \in I}^{\mathbf{v}_0} \mathbf{v}_i = \mathbf{v}_8$. Working with the complemented points given in Fig. 3(b), the supremum is $\bigvee_{i \in I}^{\mathbf{v}_0} \overline{\mathbf{v}}_i = \overline{\mathbf{v}}_9$ and the infimum is $\bigwedge_{i \in I}^{\mathbf{v}_0} \overline{\mathbf{v}}_i = \overline{\mathbf{v}}_3$, and consequently, $\bigvee_{i \in I}^{\mathbf{v}_0} \mathbf{v}_i = \overline{\bigwedge_{i \in I}^{\mathbf{v}_0} \overline{\mathbf{v}}_i}$, but nevertheless $\bigwedge_{i \in I}^{\mathbf{v}_0} \mathbf{v}_i \neq \overline{\bigvee_{i \in I}^{\mathbf{v}_0} \overline{\mathbf{v}}_i}$. If the reference is now $\mathbf{v}_0'$, we obtain for $(\mathbf{v}_i)_{i \in I}$ the supremum $\mathbf{v}_1$ and the infimum $\mathbf{v}_5$ and for $(\overline{\mathbf{v}}_i)_{i \in I}$, $\overline{\mathbf{v}}_5$ and $\overline{\mathbf{v}}_1$ respectively. Hence, the property

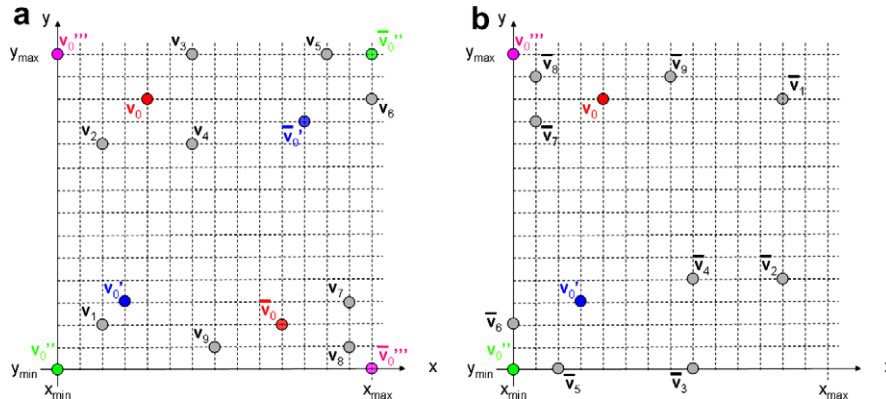

Fig. 3. Bounded vector space $[x_{min}, x_{max}] \times [y_{min}, y_{max}]$: (a) family of nine points $(\mathbf{v}_i)_{i \in I}$ and four references $\mathbf{v}_0$, $\mathbf{v}_0'$, $\mathbf{v}_0''$, $\mathbf{v}_0'''$ (and corresponding complemented references), (b) complemented points $(\overline{\mathbf{v}}_i)_{i \in I}$ and same references.

of duality is preserved. The same result is obtained for $\mathbf{v}_0'' = (x_{\min}, y_{\min})$. We can suppose based on these examples that the duality is verified when the reference is one of the extremal points or a point on the main diagonals of the space. Unfortunately this is not true in general: a counterexample is obtained by choosing as reference $\mathbf{v}_0''' = (x_{\min}, y_{\max})$ (the sup and the inf are, respectively, $\mathbf{v}_2$ and $\mathbf{v}_8$ whereas in the complemented space, the sup is $\overline{\mathbf{v}}_8$ and the inf $\overline{\mathbf{v}}_3$).

Note that one easily verifies that the duality is always valid for the orderings grounded exclusively in lexicographical cascades, without including the pre-ordering based on the distance to a reference. Incidentally, we can observe that the duality is verified for the total orderings including the reference $\mathbf{v}_0 = (x_0, y_0)$ if and only if the supremum and the infimum associated to the total distance to $\mathbf{v}_0$ are the same as the supremum and the infimum associated to the separate distances to x_0 and to y_0. In other words, a property of *separability* of both axis x and y in the computation of the distance to $\mathbf{v}_0$ is required to guarantee the duality.

In conclusion, we have the following property for colour images. If the reference colour $\mathbf{c}_0$ verifies the above property of separability for any pair of distinct points $c_i, c_j \in \mathscr{T}^{\mathrm{uvw}}$, it holds that $(c_i <_{\Omega_{c_0}} c_j) \Longleftrightarrow (\overline{c}_i >_{\Omega_{c_0}} \overline{c}_j)$. Consequently, for an erosion/dilation adjunction defined in $\mathscr{F}(E, \mathscr{T}^{\mathrm{uvw}})$ it follows then that $\varepsilon_{\Omega_{c_0}}(\mathbf{f}) = \delta_{\Omega_{c_0}}(\overline{\mathbf{f}})$. This property is named *quasi-duality* of the family of orderings given by (5).

We can also investigate the effect of computing the complement of the reference colour, or in other words, under which conditions the property $(c_i <_{\Omega_{c_0}} c_j) \overset{?}{\Longleftrightarrow} (c_i >_{\Omega_{\overline{c}_0}} c_j)$ is verified. From the example of Fig. 3(a), for $\overline{\mathbf{v}}_0$ we have that the supremum $\bigvee_{i \in I}^{\overline{\mathbf{v}}_0} \mathbf{v}_i = \mathbf{v}_7$ and the infimum $\bigwedge_{i \in I}^{\overline{\mathbf{v}}_0} \mathbf{v}_i = \mathbf{v}_3$ implies that $\bigwedge_{i \in I}^{\mathbf{v}_0} \mathbf{v}_i \neq \bigvee_{i \in I}^{\overline{\mathbf{v}}_0} \mathbf{v}_i$. Moreover, in the case $\overline{\mathbf{v}}_0'$ (or $\overline{\mathbf{v}}_0''$), the supremum is $\mathbf{v}_7$ and the infimum $\mathbf{v}_1$, and consequently the duality is not verified either. In conclusion, no property of duality seems to be associated to the complement of the reference colour.

4. Morphological colour operators

Once the family of total orderings (5) have been established, the morphological colour operators are defined in the standard way. We limit here our developments to the flat operators, i.e., the structuring elements are planar. The non-planar structuring functions are defined by weighting values on their support [44]. The implementation and the use of colour structuring functions will be the object of future research.

We need to recall a few notions which characterise the properties of morphological operators. Let ψ be an operator on a complete lattice $\mathscr{F}(E, \mathscr{T}^{\mathrm{uvw}})$. ψ is increasing if $\forall \mathbf{f}, \mathbf{g} \in \mathscr{F}(E, \mathscr{T}^{\mathrm{uvw}})$, $\mathbf{f} \leqslant_\Omega \mathbf{g} \Rightarrow \psi(\mathbf{f}) \leqslant_\Omega \psi(\mathbf{f})$. It is anti-extensive if $\psi_\Omega(\mathbf{f}) \leqslant_\Omega \mathbf{f}$ and it is extensive if $\mathbf{f} \leqslant_\Omega \psi_\Omega(\mathbf{f})$. An operator is idempotent if it is verified that $\psi(\psi(\mathbf{f})) = \psi(\mathbf{f})$.

4.1. Erosion and dilation

The *colour erosion* of an image $\mathbf{f} \in \mathscr{F}(E, \mathscr{T}^{\mathrm{uvw}})$ at pixel $x \in E$ by the structuring element $B \subset E$ of size n is given by

$$\varepsilon_{\Omega, nB}(\mathbf{f})(x) = \{\mathbf{f}(y) : \mathbf{f}(y) = \wedge_\Omega[\mathbf{f}(z)], z \in n(B_x)\}, \quad (6)$$

where $\inf_\Omega$ is the infimum according to the total ordering Ω. The corresponding *colour dilation* $\delta_{\Omega, nB}$ is obtained by replacing the $\inf_\Omega$ by the $\sup_\Omega$, i.e.,

$$\delta_{\Omega, nB}(\mathbf{f})(x) = \{\mathbf{f}(y) : \mathbf{f}(y) = \vee_\Omega[\mathbf{f}(z)], z \in n(B_x)\}. \quad (7)$$

The erosion and the dilation are increasing operators. Moreover, the erosion is anti-extensive and the dilation is extensive. In practice, the colour erosion shrinks the structures which have a colour close to the reference; "peaks of colour" thinner than the structuring element disappear by taking the colour of neighboring structures with a colour away from the reference. As well, it expands the structures which have a colour far from the reference. Dilation produces the dual effects, enlarging the regions having a colour close to the reference and contracting the others.

4.2. Morphological filters

In general, a morphological filter is an increasing operator that is also idempotent (the erosion/dilation are not idempotent).

4.2.1. Opening and closing
A *colour opening* is an erosion followed by a dilation, i.e.,

$$\gamma_{\Omega, nB}(\mathbf{f}) = \delta_{\Omega, nB}(\varepsilon_{\Omega, nB}(\mathbf{f})), \quad (8)$$

and a *colour closing* is a dilation followed by an erosion, i.e.,

$$\varphi_{\Omega, nB}(\mathbf{f}) = \varepsilon_{\Omega, nB}(\delta_{\Omega, nB}(\mathbf{f})). \quad (9)$$

The opening (closing) is an anti-extensive (extensive) operator. More precisely, the opening removes colour peaks that are thinner than the structuring element, having a colour close to the reference; the closing remove colour peaks that are thinner than the structuring element, having a colour far from the reference.

4.2.2. Alternate sequential filters
Once the colour opening and closing are defined it is indubitable how to extend other classical operators such as the *colour alternate sequential filters* (or ASF), obtained by concatenation of openings and closings, i.e.,

$$ASF(\mathbf{f})_{\Omega, nB} = \varphi_{\Omega, nB} \gamma_{\Omega, nB} \cdots \varphi_{\Omega, 2B} \gamma_{\Omega, 2B} \varphi_{\Omega, B} \gamma_{\Omega, B}(\mathbf{f}). \quad (10)$$

A dual family of ASF operators is obtained by changing the order of the openings/closings. The ASF act simultaneously on the peaks and the valleys, simplifying (smoothing) them. They are useful when dealing with noisy signals.

4.2.3. Contrast mappings
The contrast mapping is a particular operator from a more general class of transformations called toggle

mappings [45]. A contrast mapping is defined, on the one hand, by two primitives ϕ_1 and ϕ_2 applied to the initial function, and on the other hand, by a decision rule which makes, at each point x the output of this mapping toggles between the value of ϕ_1 at x and the value of ϕ_2, according to which is closer to the input value of the function at x. If the primitives are an erosion $\varepsilon_{\Omega,nB}(\mathbf{f})$ and the adjunction dilation $\delta_{\Omega,nB}(\mathbf{f})$, the *colour contrast mapping* for an image $\mathbf{f}$ is given by [26]:

$$\kappa_{\Omega,nB}^{\varepsilon\delta}(\mathbf{f})(x) = \begin{cases} \delta_{\Omega,nB}(\mathbf{f})(x) & \text{if} \quad \|\mathbf{f}(x) - \delta(\mathbf{f})(x)\| \leqslant \|\mathbf{f}(x) - \varepsilon(\mathbf{f})(x)\| \\ \varepsilon_{\Omega,nB}(\mathbf{f})(x) & \text{if} \quad \|\mathbf{f}(x) - \delta(\mathbf{f})(x)\| > \|\mathbf{f}(x) - \varepsilon(\mathbf{f})(x)\| \end{cases} \tag{11}$$

where $\delta(\mathbf{f})$ and $\varepsilon(\mathbf{f})$ of the norms correspond to $\delta_{\Omega,nB}(\mathbf{f})$ and $\varepsilon_{\Omega,nB}(\mathbf{f})$ respectively. Usually, the norm used to compute the distance in the contrast mappings is the same as the norm applied in the Ω-ordering associated to the colour erosion/dilation. This morphological transformation enhances the local contrast of $\mathbf{f}$ by sharpening its colour edges. It is usually applied more than once, being iterated, and the iterations converge to a limit reached after a finite number of iterations. Another interesting colour contrast mapping $\kappa_{\Omega,nB}^{\gamma\varphi}(\mathbf{f})$ is defined by changing in the previous expression the pair of colour erosion/dilation by a colour opening $\gamma_{\Omega,nB}(\mathbf{f})$ and the dual closing $\varphi_{\Omega,nB}(\mathbf{f})$ [33]. This second contrast operator is idempotent but a decreasing transformation (it cannot be considered strictly as a morphological filter). More recently, these sharpening methods are called shock filters [38].

4.2.4. Morphological centre

The opening/closing are non-linear smoothing filters, and classically an opening followed by a closing (or a closing followed by an opening) can be used to suppress impulse noise, i.e., suppressing positive spikes via the opening and negative spikes via the closing and without blurring the contours. However, the results are usually not satisfactory. A more interesting operator to suppress colour noise is the morphological centre, also known as automedian filter [44,45]. Given an opening $\gamma_{\Omega}(\mathbf{f})$ and the dual closing $\varphi_{\Omega}(\mathbf{f})$ with a small structuring element (typically square of size equal to the "noise size"), the *colour morphological centre* associated to these primitives for an image $\mathbf{f}$ is given by the algorithm:

$$\zeta_{\Omega}(\mathbf{f}) = [f \vee_{\Omega} (\gamma\varphi\gamma(\mathbf{f}) \wedge_{\Omega} \varphi\gamma\varphi(\mathbf{f}))] \wedge_{\Omega} (\gamma\varphi\gamma(\mathbf{f}) \vee_{\Omega} \varphi\gamma\varphi(\mathbf{f})). \tag{12}$$

This is an increasing and autodual operator, not idempotent, but the iteration of ζ presents a point monotonicity and converges to the idempotence, i.e., $\widehat{\zeta}_{\Omega}(\mathbf{f}) = [\zeta_{\Omega}(\mathbf{f})]^i$, such that $[\zeta]^i = [\zeta]^{i+1}$.

4.2.5. Residue-based operators

Moreover, using a colour distance to calculate the image distance d, $d \in \mathscr{F}(E, \mathscr{T})$ (a scalar function), given by the difference point-by-point of two colour images $d(x) = \|\mathbf{f}(x)\text{-}\mathbf{g}(x)\|$, we can easily define the *morphological colour gradient*, i.e.,

$$\varrho_{\Omega}(\mathbf{f}) = \|\delta_{\Omega,B}(\mathbf{f}) - \varepsilon_{\Omega,B}(\mathbf{f})\|. \tag{13}$$

This function gives the contours of the image, attributing more importance to the transitions between regions close/far to the colour reference. For the sake of coherence, the norm used for the distance d is the same as the norm applied in the ordering Ω associated with the corresponding colour operator. However, another different colour norm can also be considered.

The *positive colour top-hat transformation* is the residue of a colour opening, i.e.,

$$\rho_{\Omega,nB}^+(\mathbf{f}) = \|\mathbf{f} - \gamma_{\Omega,nB}(\mathbf{f})\|. \tag{14}$$

Dually, the *negative colour top-hat transformation* is given by

$$\rho_{\Omega,nB}^-(\mathbf{f}) = \|\varphi_{\Omega,nB}(\mathbf{f}) - \mathbf{f}\|. \tag{15}$$

The top-hat transformation yields grey-level images and is used to extract contrasted components with respect to the background, where the background corresponds to the structures far from the reference. Moreover, top-hats remove the slow trends, and thus enhancing the contrast of objects smaller than the structuring element used for the opening/closing.

4.3. Geodesic reconstruction, derived operators, leveling

In addition, we also propose the extension of operators "by reconstruction", implemented using the geodesic dilation. The *colour geodesic dilation* is based on restricting the iterative dilation of a function marker $\mathbf{m}$ by B to a function reference $\mathbf{f}$ [53], i.e.,

$$\delta_{\Omega}^n(\mathbf{m}, \mathbf{f}) = \delta_{\Omega}^1 \delta_{\Omega}^{n-1}(\mathbf{m}, \mathbf{f}), \tag{16}$$

where the unitary conditional dilation is given by $\delta_{\Omega}^1(\mathbf{m}, \mathbf{f}) = \delta_{\Omega,B}(\mathbf{m}) \wedge_{\Omega} \mathbf{f}$. Typically, B is an isotropic structuring element of size *1*.

The *colour reconstruction* by dilation is then defined by

$$\gamma_{\Omega}^{\text{rec}}(\mathbf{m}, \mathbf{f}) = \delta_{\Omega}^i(\mathbf{m}, \mathbf{f}), \tag{17}$$

such that $\delta_{\Omega}^i(\mathbf{m}, \mathbf{f}) = \delta_{\Omega}^{i+1}(\mathbf{m}, \mathbf{f})$ (idempotence). Whereas the adjunction opening $\gamma_{\Omega,nB}(\mathbf{f})$ (from an erosion/dilation) modifies the colour contours, the associated opening by reconstruction $\gamma_{\Omega}^{\text{rec}}(\mathbf{m}, \mathbf{f})$ (where the marker $\mathbf{m} = \varepsilon_{\Omega,nB}(\mathbf{f})$ or $\mathbf{m} = \gamma_{\Omega,nB}(\mathbf{f})$) is aimed at efficiently and precisely reconstructing the contours of the colour objects having a colour close to the reference and which have not been totally removed by the marker filtering process.

In a similar way, the *colour leveling* $\lambda_{\Omega}(\mathbf{m},\mathbf{f})$ of a reference function $\mathbf{f}$ and a marker function $\mathbf{m}$ is a symmetric geodesic operator computed by means of an iterative algorithm with geodesic dilations and geodesic erosions until idempotence [34], i.e.,

$$\lambda_{\Omega}(\mathbf{m}, \mathbf{f})^i = [\mathbf{f} \wedge_{\Omega} \delta_{\Omega}^i(\mathbf{m})] \vee_{\Omega} \varepsilon_{\Omega}^i(\mathbf{m}), \tag{18}$$

until $\lambda_{\Omega}(\mathbf{m},\mathbf{f})^i = \lambda_{\Omega}(\mathbf{m},\mathbf{f})^{i+1}$. The leveling simplifies the colour image, removing the objects and textures smaller than the

structuring element and preserving the contours of the remaining objects. Moreover, it acts simultaneity on the "positive objects" (i.e., having a colour close to the reference) and "negative objects" (i.e., colour far from the reference).

5. Results and discussion

We explore in this section the effects of these morphological operators when they are applied to colour images according to the family of orderings introduced in this paper. We try to illustrate a wide variety of morphological

colour operators with different colour spaces, distances and colour references. As mentioned, the present approach generalises other orderings proposed in the literature. Even if we are conscious of the fact that a further study would need more extensive comparisons, we consider that the following comparative examples allow us to draw some interesting conclusions.

Fig. 4 gives a first comparison of the results obtained for the image "Baboon", when the same operator, a colour opening by reconstruction $\gamma_\Omega(\mathbf{f})$, is applied using different orderings. It is observed that the results are absolutely
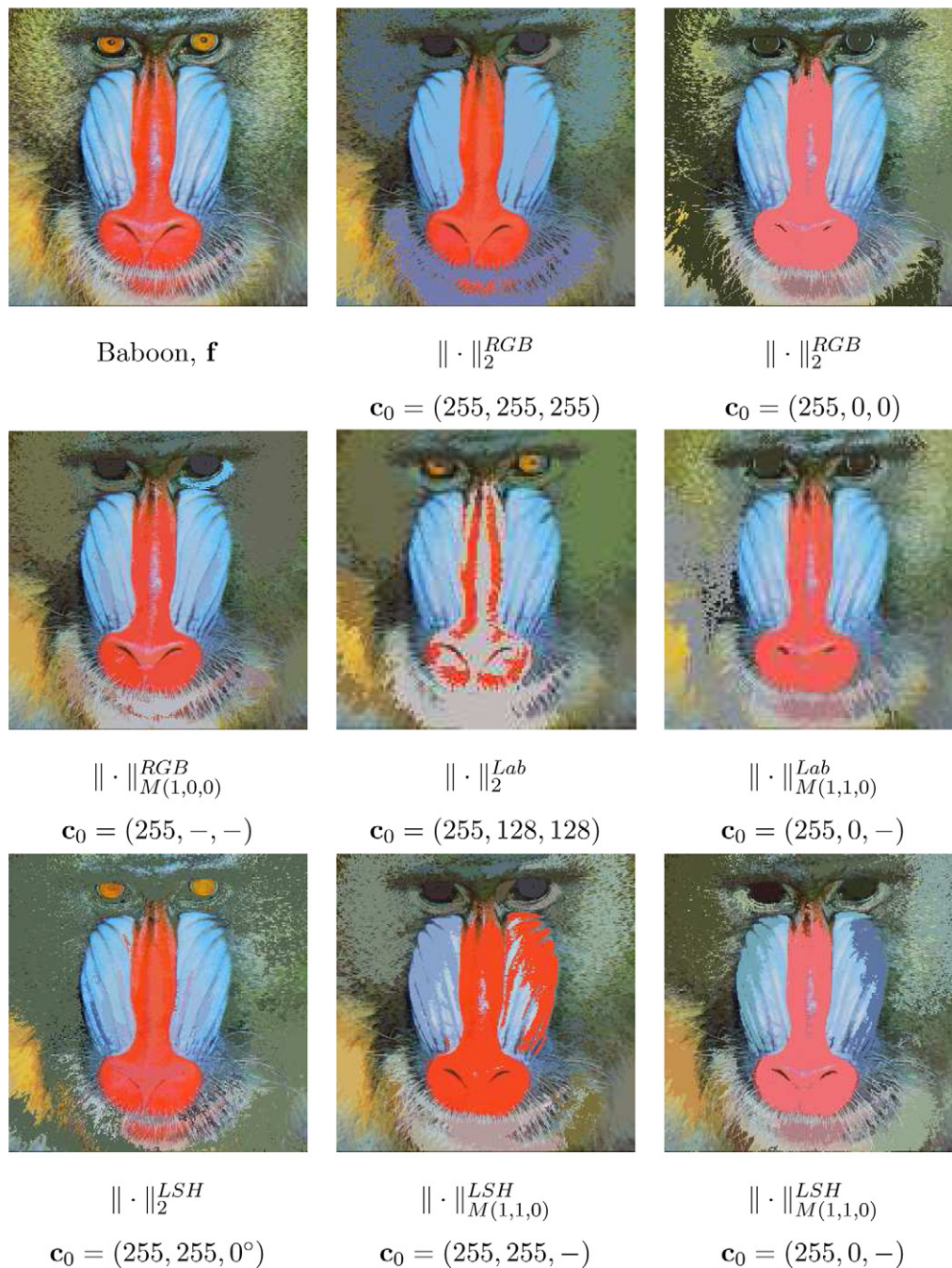

Baboon, $\mathbf{f}$

$\| \cdot \|_2^{RGB}$
$\mathbf{c}_0 = (255, 255, 255)$

$\| \cdot \|_2^{RGB}$
$\mathbf{c}_0 = (255, 0, 0)$

$\| \cdot \|_{M(1,0,0)}^{RGB}$
$\mathbf{c}_0 = (255, -, -)$

$\| \cdot \|_2^{Lab}$
$\mathbf{c}_0 = (255, 128, 128)$

$\| \cdot \|_{M(1,1,0)}^{Lab}$
$\mathbf{c}_0 = (255, 0, -)$

$\| \cdot \|_2^{LSH}$
$\mathbf{c}_0 = (255, 255, 0°)$

$\| \cdot \|_{M(1,1,0)}^{LSH}$
$\mathbf{c}_0 = (255, 255, -)$

$\| \cdot \|_{M(1,1,0)}^{LSH}$
$\mathbf{c}_0 = (255, 0, -)$

Fig. 4. Comparison of colour opening by reconstruction $\gamma_\Omega^{\text{rec}}(\mathbf{f})$ for the image $\mathbf{f}$ "Baboon" (the marker is an erosion $\varepsilon_{\Omega, nB}(\mathbf{f})$ where the structuring element B is a square of size $n = 20$) according to different distance-based total orderings.

different according to the distance-based total ordering chosen. We show only examples for the L_2 and the Mahalanobis distance. As expected, the orderings based on L_∞ produce very unsatisfactory visual results and the results for L_1 norm distances are almost equal to the results achieved using L_2. Note also the flexibility of the approach: for instance, in RGB the result of the opening for L_2 distance to the origin (255,0,0) (pure red), which suppresses all the small red objects, is very different from the Mahalonobis distance with weights (1,0,0) (the R component is exclusively considered) to the same origin, which suppresses the bright objects according only the red component. On the other hand, we observe that the orderings with distances including chromatic components (i.e., h, a* and b*) produce poor results. Moreover the choice of the origin is not easily understandable for the a* and b* components (chromatic axis of opposite colours). Even if the Euclidean distance in the L*a*b* colour space has interesting perceptual properties, we remark that for the implementation of morphological operators the most important issue is in fact the choice of the origin. Hence, the use of the L_2 distance in LSH or L*a*b* should be considered for feature extraction operators according to a specific reference colour. We remark also that in order to remove all the bright structures of a natural colour image by means of an opening, the results are more satisfactory from a visual point of view for $\|\cdot\|_2^{RGB}$, $\mathbf{c}_0 = (255,255,255)$ than for $\|\cdot\|_{M(1,1,0)}^{LSH}$, $\mathbf{c}_0 = (255,255,-)$.

In order to illustrate the effect of geodesic operators, Fig. 5 gives an example of colour "swamping" or reconstruction of a function by imposing markers for the maxima (to remove the useless maxima). In this case, the one-point marker is a pixel on the big bear ("mrk 1" touches the dark part of the fur), which value in RGB is approximately (140,120,100). Working in RGB and using L_2 distance, we observe that, if the reference colour is (255,255,255), the propagation from the marker imposes that any other pixel must have a colour whose distance to the reference (maximal luminance) is longer than the distance of the marker to the reference. Consequently, there is not any pixel upper intensities RGB other than the marker. When the reference colour matches with the marker, $\mathbf{c}_0 = (140,120,100)$, the marked object is preserved and

moreover, the other regions with the same colour are removed (only one maxima after this swamping transformation remains). In this case, the dark part of the fur is again preserved and the objects which have a colour very distant from the marker are also preserved (bright part of the image).

Fig. 6 shows the comparison of different colour levelings for the simplification of image "Lenna", where the markers are ASF. We observe that the degree of simplification (i.e., which structures are preserved and which structures are removed) is relatively equivalent for the different orderings; and the differences between the orderings are associated to the final colours of simplified structures. We again remark that the visual results for $\|\cdot\|_2^{RGB}$, $\mathbf{c}_0 = (255,255,255)$ are slightly better than for $\|\cdot\|_{M(1,1,0)}^{LSH}$, $\mathbf{c}_0 = (255,255,-)$. It is also shown how a part of the image structures can be harshly leveled (the violet part of the hat) by imposing their colour as reference, i.e., (100,50,100).

In Fig. 7 the use of colour residue-based operators is compared for detail extraction. In RGB, a closing is given for L_2 distance and $\mathbf{c}_0 = (255,255,255)$, and the corresponding residue (i.e., black top-hat) with the same distance, which extracts the dark details (the letters of panels and a part of the texture). We observe that, if we fix $\mathbf{c}_0 = (0,0,0)$, we obtain by black top-hat the bright details (the interstices between the letters and the "positive" parts of textures). Here, we found the usefulness of quasi-duality property since the residue of a closing with $\mathbf{c}_0 = (0,0,0)$ is approximately equivalent to the residue of an opening with $\mathbf{c}_0 = (255,255,255)$. Once again, the result for RGB is compared with $\|\cdot\|_{M(1,1,0)}^{LSH}$, $\mathbf{c}_0 = (255,255,-)$, without observing substantial differences.

Fig. 8 depicts an example of colour segmentation by inner/outer markers-driven watershed transformation [9]. In this example the aim is to define the contour of the horse, and hence the inner marker is a segment going through the horse and the outer marker is the image border. The different colour gradients are then used with the watershed transformation. This example is particularly interesting to show the importance of the choice of the gradient for colour segmentation. The colour of the horse is variable with approximately RGB value of (250,110,90)
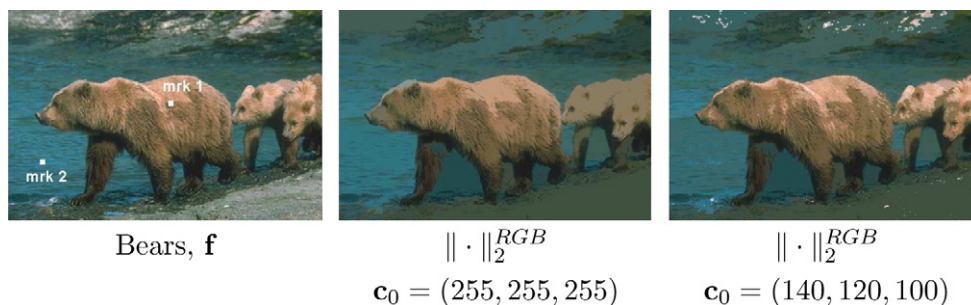

Bears, $\mathbf{f}$ $\qquad$ $\|\cdot\|_2^{RGB}$ $\qquad$ $\|\cdot\|_2^{RGB}$

$\mathbf{c}_0 = (255,255,255)$ $\qquad$ $\mathbf{c}_0 = (140,120,100)$

Fig. 5. Example of colour swamping for the image "Bears", where the one-point marker is a pixel on the fur ("mrk 1"), which value in RGB is approximately (140,120,100).
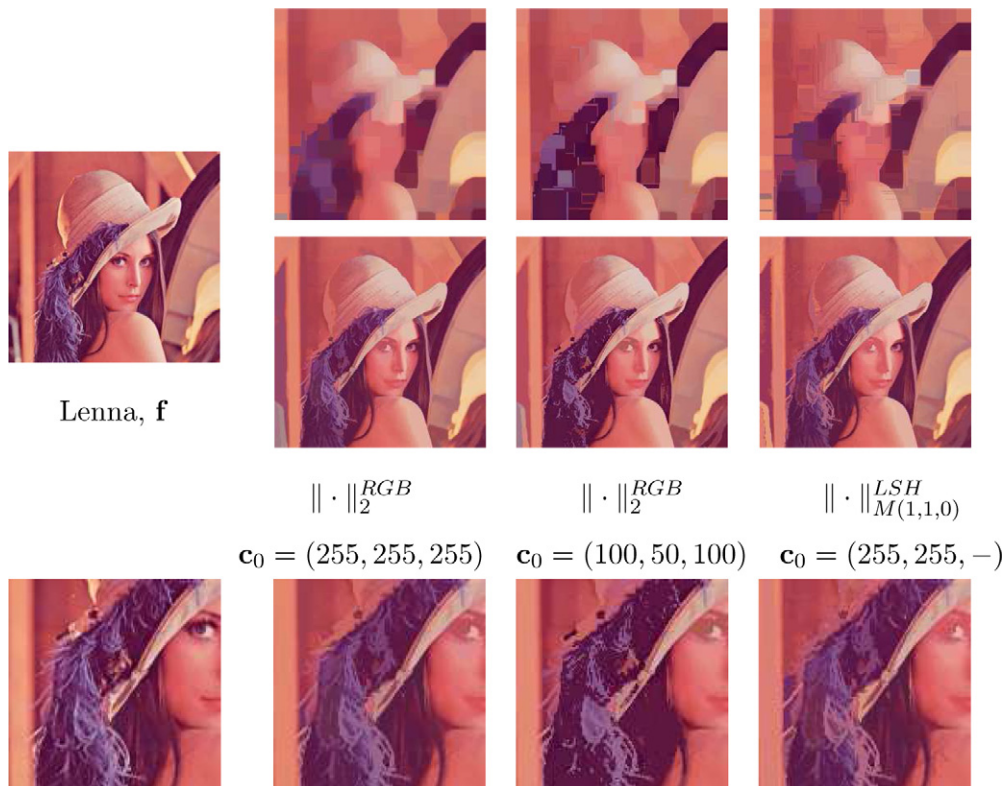
Fig. 6. Comparison of colour leveling $\lambda_\Omega(\mathbf{f})$ for the image $\mathbf{f}$ "Lenna" according to different distance-based total orderings. Upper row, the marker is an ASF, $ASF_{\Omega,nB}(\mathbf{f})$, where the structuring element B is a square of size $n = 15$; lower row, the corresponding levelings. At the bottom are zoom-in frames of a square section cropped from the initial (left) leveled images.
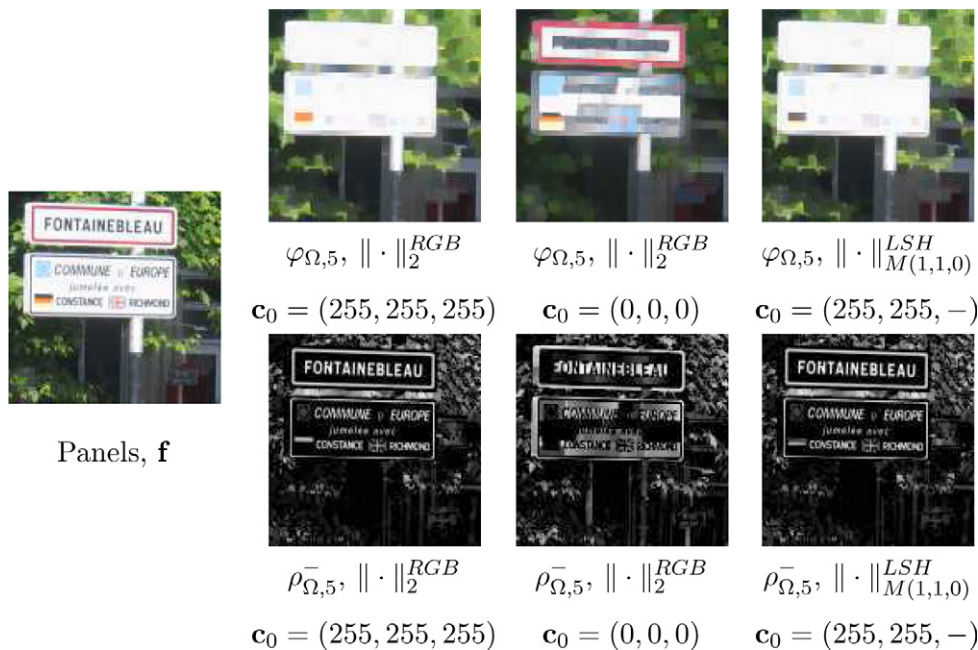

Fig. 7. Colour details extraction of image "Panels". Upper row, square closing of size 5×5 pixels; lower row, the associated negative top-hats.

or LSH value of (180,128,0°). We observe that, even if the results in RGB or LSH are better when the reference $\mathbf{c}_0$ equals the horse colour than the maximal value, the obtained segmentation is not satisfactory. In fact, the horse has an homogenous hue (around 10°) but a variable luminance and saturation (similar to the values of luminance
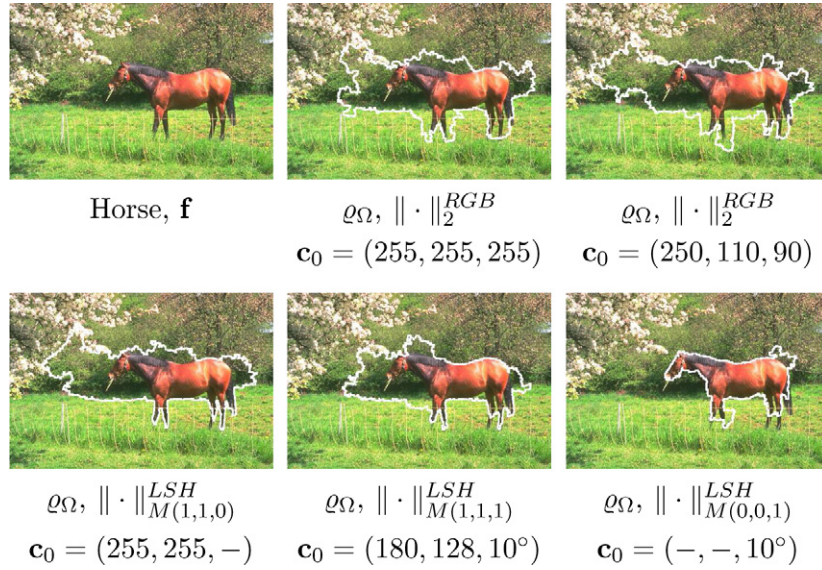
Fig. 8. Application of colour gradients for watershed-based segmentation of image "Horse". The white contour corresponds to the region obtained using an inner marker for the horse region (the outer marker is the image border).
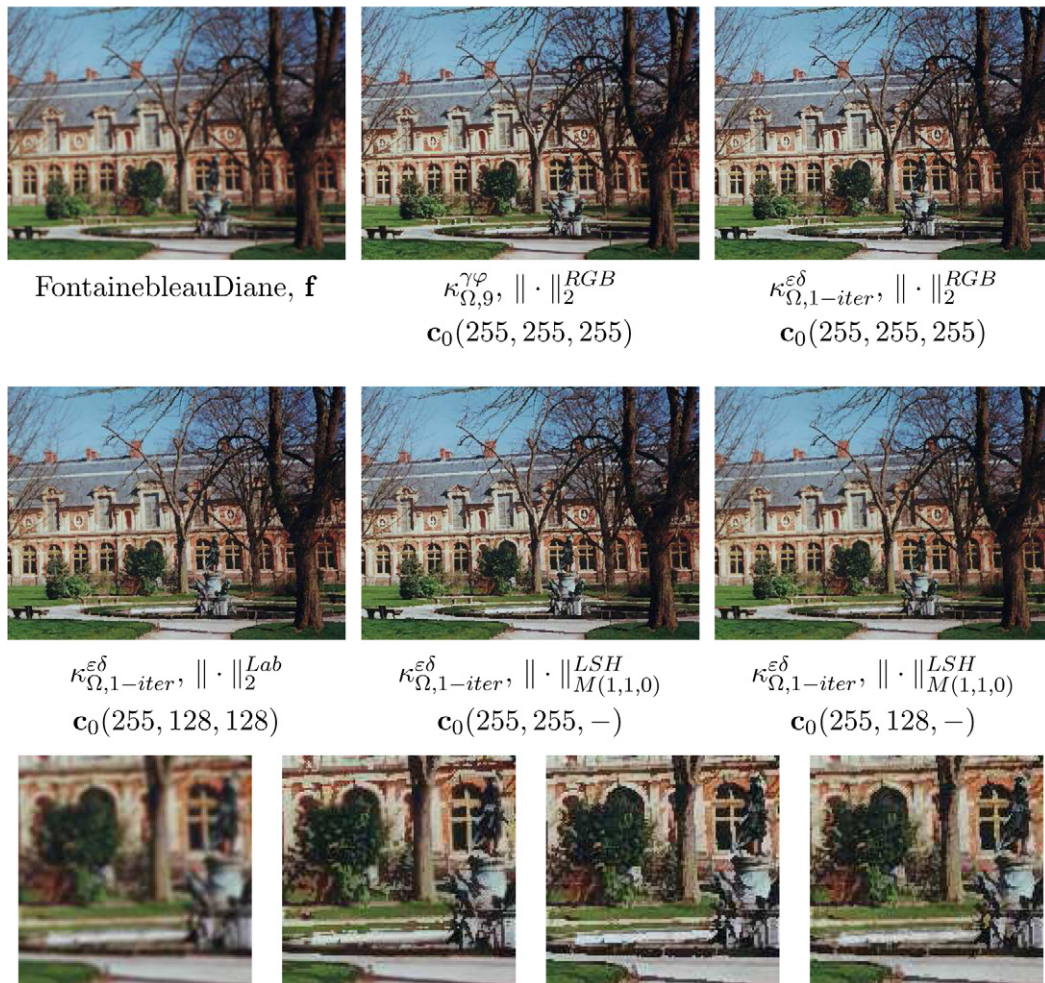

Fig. 9. Contrast enhancement of colour image "FontainebleauDiane" using the contrast mapping κ. At the bottom are zoom-in frames of a square section cropped from the initial (left) and three of enhanced images (using $\kappa_{\Omega,9}^{\gamma\varphi}$ in RGB, $\kappa_{\Omega,1-iter}^{\varepsilon\delta}$ in RGB and $\kappa_{\Omega,1-iter}^{\varepsilon\delta}$ in LSH with $\mathbf{c}_0(255,128,-)$, respectively).

and saturation of background). Therefore, a gradient exclusively using the hue component (distance $\| \cdot \|_{M(0,0,1)}^{LSH}$ and reference $c_0(-,-,10°)$) yields the best result.

Fig. 9 shows a comparative example of contrast enhancement of the blurred image "FontainebleauDiane". The blur involves a Gaussian filter with $\sigma = 5$. It is well known that, in order to have significant enhancement, the size of contrast mapping based on opening/closing $\kappa^{\gamma\varphi}$ must be considerable and that it can involve visual artefacts. For this example, the size $n = 9$ seems to be a trade-off to obtain a perceptible enhancement. In fact, the effects obtained are in general better for the iteration of $\kappa^{\varepsilon\delta}$. Concerning the distance-based total ordering, it seems that for this example the best visual result is associated with the choice $\| \cdot \|_{M(1,1,0)}^{LSH}$, $c_0(255,128,-)$, which enhances the bright/dark structures, with an intermediate saturation (chromatic and achromatic simultaneously) and independently from the hue.

In Fig. 10 is given an example of morphological centre to filter colour noise. The image "CarmenBianca" has been corrupted by adding salt-and-pepper noise on the hue component (occurring with probability 0.05) and where the luminance for noise pixels is maximal and the saturation

is half. As we can observe, for this noise distribution, the results are better using only the luminance component ($\| \cdot \|_{M(1,0,0)}^{LSH}$, $c_0(255,-,-)$) than the RGB components ($\| \cdot \|_2^{RGB}$, $c_0(255,255,255)$). Note also that the result associated with the opening-closing operator for a size equal to the centre is worse in terms of noise suppression. We show in the zoom-in images the results of an equivalent marginal RGB median which suppresses the noise but rounds off the colour contours. The result for $\| \cdot \|_{M(1,1,0)}^{LSH}$, $c_0(255,128,-)$, which corresponds to the noise distribution properties, is relatively satisfactory. In fact, it seems that the flexible choice of a particular distance and a colour reference can be interesting in order to obtain optimal filters for a particular distribution of noise. The challenge lies in estimating the statistical colour noise properties, so that the Mahalanobis distance is naturally well adapted to this problem (applying an estimated covariance matrix Γ).

As a matter of fact, we cannot conclude from the qualitative analysis of these examples that a specific ordering is more suitable for one operator or another. In fact, we believe that it is not possible to assert which ordering is more appropriate for a given morphological operator.
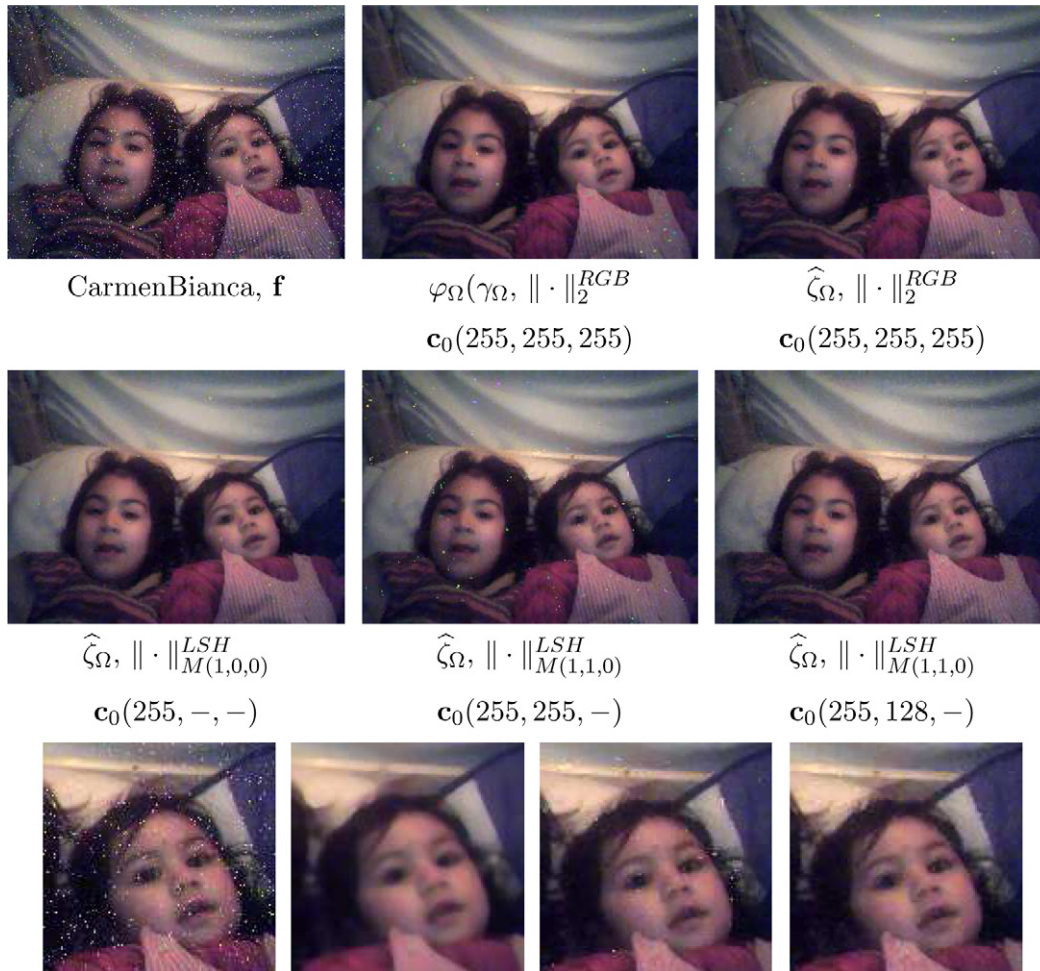

Fig. 10. Denoising of colour image "CarmenBianca" using the morphological centre $\widehat{\zeta}$. At the bottom are zoom-in frames of a square section cropped from the initial (left), a marginal median (in RGB of equivalent size) and two of centered images (using $\widehat{\zeta}_\Omega$ in LSH with $c_0(255,255,-)$ and $c_0(255,128,-)$ respectively).

The right choice of a colour distance and a colour reference depends on the nature of the image, the features of the target structures, as well as the properties of the operation applied, and others. For instance, using only one image we cannot determine the best gradient for colour segmentation. However, using a database of manually segmented images we can evaluate the segmentation obtained with the different gradients and determine the best gradient for the type of images. In addition, machine learning techniques can be applied to automatically adapt the best parameters for a specific problem.

5.1. Application to biomedical microscopic colour images

To complement the experimental part of this article, we propose to illustrate the application of morphological colour operators to biomedical microscopic colour images. In biomedicine, the microscopic samples (tissues, cells, proteins, etc.) are classically fixed and stained by different chemical components, in order to enhance the interesting structures with a particular colour [10]. In addition, recent advances in molecular biology allow to mark specific targets with fluorochrome probes [49]. The application of colour processing to these images is an active field.

Fig. 11 gives the example of colour analysis of an image with cells marked with dark violet, located on a heterogeneous tissue (marked bright yellow and pink). The aim of this processing is to separate the cells and the tissue to make easier the later quantification of both elements (count cells, evaluate cell aggregation, study the distribution of colour pink/yellow on the tissue, etc.). The dichotomy dark/bright implies the use of luminance information; moreover the different colour elements present a similar

saturation. Hence, the two "colour phases" are extracted by closing/opening by reconstruction using the ordering based on $\| \cdot \|_{M(1,0.2,0)}^{LSH}$, $\mathbf{c}_0(255,128,-)$. Even if the saturation has a low contribution, we have observed that the result is better where the luminance information also includes the saturation information. For the tissue, the marker is a dilation of 25, which removes the dark structures and by dual reconstruction recovers the tissue contours. In the case of cells, the marker is an erosion of size 75 which propagates the cell colour followed by the reconstruction that fills up the background.

Fig. 12 shows the successive steps of an example of analysis for a Cy3/Cy5 cDNA microarray images [11,3]. From the viewpoint of this paper, a cDNA microarray image is a two-channel Red–Green image (it can be seen as an RGB image with zero blue component) consisting of green, red and yellow spots. The goal of microarray image analysis is to locate and segment the spots and to quantify the intensity for each spot. Since microarray images are usually very noisy, image filtering and enhancement [29,30] are required in order to increase the accuracy of the subsequent analysis processes. Our aim in the particular example of Fig. 12 is to extract the spots marked with red fluorescence (pure red and yellow spots). Firstly, the image f is pre-filtered by means of the contrast and centre operators (to remove the noise and to enhance the spot contours), followed by an opening by reconstruction of size 3 (to regularise the spots, by removing the intensity structures of size lower that 3×3 pixels). Both transformations are based on the luminance/saturation processing ($\| \cdot \|_{M(1,1,0)}^{LSH}$, $\mathbf{c}_0(255,128,-)$). Then, the reconstruction using as marker an erosion of size 15 (rough estimate of spot diameter) removes the spots which has a pure green colour
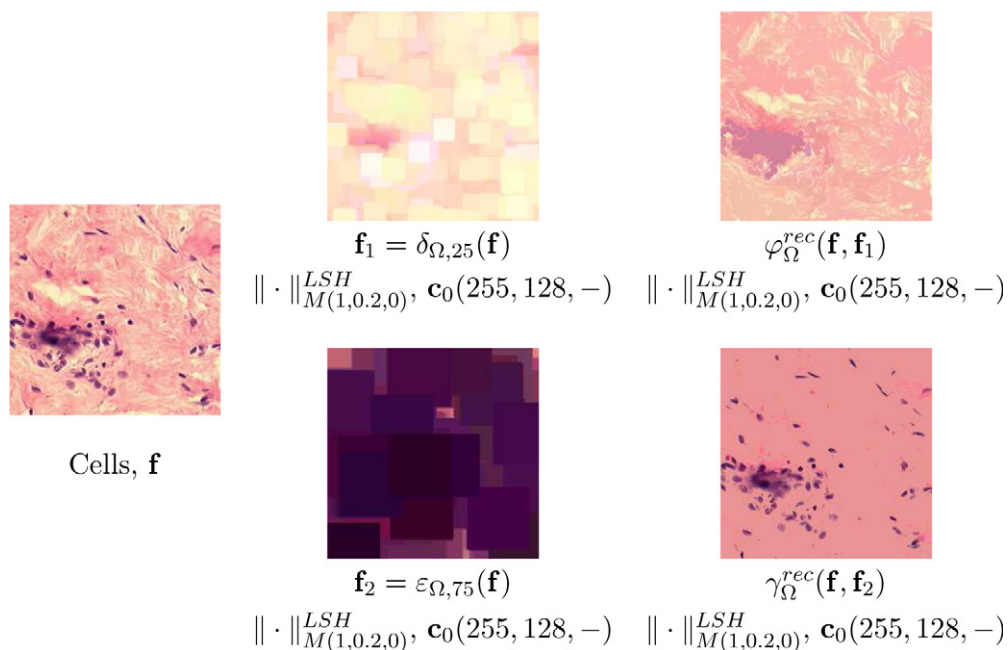

Cells, $\mathbf{f}$

$\mathbf{f}_1 = \delta_{\Omega,25}(\mathbf{f})$
$\| \cdot \|_{M(1,0.2,0)}^{LSH}$, $\mathbf{c}_0(255,128,-)$

$\varphi_{\Omega}^{rec}(\mathbf{f},\mathbf{f}_1)$
$\| \cdot \|_{M(1,0.2,0)}^{LSH}$, $\mathbf{c}_0(255,128,-)$

$\mathbf{f}_2 = \varepsilon_{\Omega,75}(\mathbf{f})$
$\| \cdot \|_{M(1,0.2,0)}^{LSH}$, $\mathbf{c}_0(255,128,-)$

$\gamma_{\Omega}^{rec}(\mathbf{f},\mathbf{f}_2)$
$\| \cdot \|_{M(1,0.2,0)}^{LSH}$, $\mathbf{c}_0(255,128,-)$

Fig. 11. Analysis of the colour image "Cells". See the text for details.

$$\mathbf{f}_1 = \widehat{\zeta}_\Omega(\kappa_{\Omega,1-iter}^{\varepsilon\delta}(\mathbf{f}))$$
$$\|\cdot\|_{M(1,1,0)}^{LSH}, \; \mathbf{c}_0(255,128,-)$$

$$\mathbf{f}_2 = \gamma_\Omega^{rec}(\mathbf{f}, \varepsilon_{\Omega,3}(\mathbf{f}_1))$$
$$\|\cdot\|_{M(1,1,0)}^{LSH}, \; \mathbf{c}_0(255,128,-)$$

cDNA-Microarray, $\mathbf{f}$

$$\mathbf{f}_3 = \varepsilon_{\Omega,15}(\mathbf{f_2})$$
$$\|\cdot\|_2^{RGB}, \; \mathbf{c}_0(0,128,255)$$

$$\mathbf{f}_4 = \gamma_\Omega^{rec}(\mathbf{f}, \mathbf{f}_3)$$
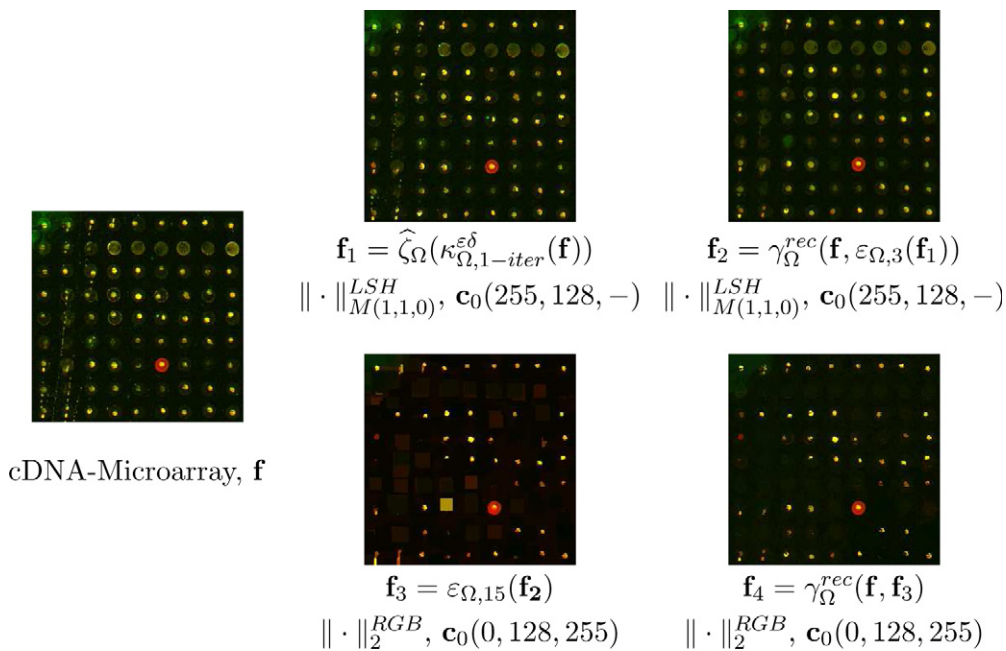$$\|\cdot\|_2^{RGB}, \; \mathbf{c}_0(0,128,255)$$

Fig. 12. Successive steps of the analysis of the colour image "cDNA-Microarray". See the text for details.

$(\|\cdot\|_2^{\mathrm{RGB}}, \mathbf{c}_0(0,128,255))$. The output image $\mathbf{f}_4$ can be used to specifically segment the red/yellow spots.

Fig. 13 illustrates an example of fluorescence-marked cell segmentation in high content screening. For this kind of applications, the touching cells must be separated in order to be able to individually analyse each cell. To apply the watershed segmentation a colour gradient is needed as well as the markers for each cell. A gradient f_g calculated using the red and green component, $\|\cdot\|_{M(2,1,0)}^{\mathrm{RGB}}$, $\mathbf{c}_0(255,255,-)$, allows defining the main contours of cells (the blue component introduces an additional contour for the cell nuclei). An opening by reconstruction of size 20

is then applied on the colour image $\mathbf{f}$ to remove the structures associated to the nuclei. The colour difference in RGB between the filtered image $\mathbf{f}_2$ and the original one $\mathbf{f}$ yields a grey-level image with the nuclei. The markers for each cell f_{mrks} are then obtained by computing the maxima of structures having a minimal diameter of 10 (using an isotropic opening). The watershed transformation of f_g and f_{mrks} provides the cell contours.

The last study-case of Fig. 14 gives another example of colour cell segmentation using the watershed transformation. Two classes of cells are presented in the image (colours brown and blue). In addition, the image $\mathbf{f}$ is very

"Hepatocytes", $\mathbf{f}$

$$f_g = \varrho_\Omega(\mathbf{f})$$
$$\|\cdot\|_{M(2,1,0)}^{RGB}, \; \mathbf{c}_0(255,255,-)$$

$$\mathbf{f}_1 = \gamma_\Omega^{rec}(\mathbf{f}, \varepsilon_{\Omega,20}(\mathbf{f}))$$
$$\|\cdot\|_2^{RGB}, \; \mathbf{c}_0(255,255,255)$$

$$f_2 = \|\mathbf{f} - \mathbf{f}_1\|_2^{RGB}$$

$$f_{mrks} = Max(\gamma_{10}(f_2))$$
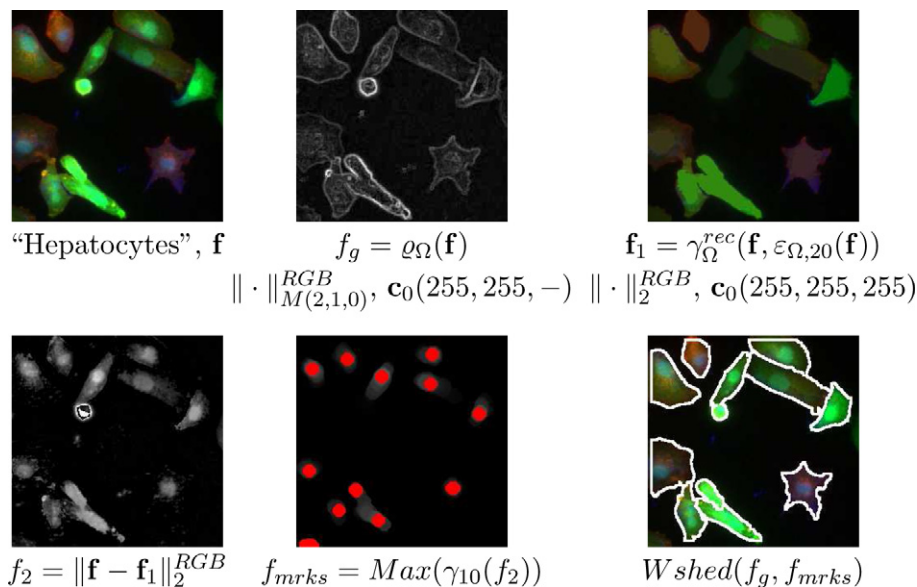
$$Wshed(f_g, f_{mrks})$$

Fig. 13. Successive steps of the analysis of the colour image "Cells2". See the text for details.
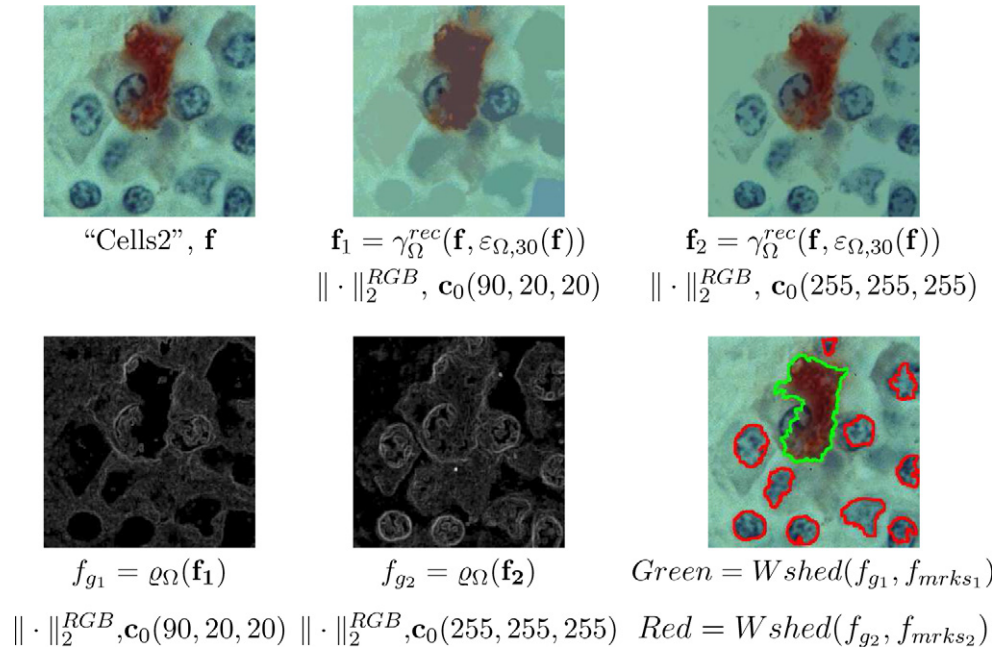
Fig. 14. Successive steps of the analysis of the colour image "Cells2". See the text for details.

textured and it is suggested to simplify the structure before computing the gradients. In this case, a first simplification $\mathbf{f}_1$ is obtained from an opening by reconstruction working on the brown structures ($\| \cdot \|_2^{\text{RGB}}$, $\mathbf{c}_0(90,20,20)$) and a second simplified image $\mathbf{f}_2$ removing the bright structures ($\| \cdot \|_2^{\text{RGB}}$, $\mathbf{c}_0(255,255,255)$). With the same orderings, a morphological gradient is calculated for each image. The gradient $\mathbf{f}_1$ is used to obtain the contours of brown cells and the gradient of $\mathbf{f}_2$ the contours of blue cells. Here, the markers for each cell are obtained using a similar approach to the previous example.

6. Conclusions and perspectives

In this study, we have introduced an algorithmic framework to apply, in a reliable and generic way, mathematical morphology operators to colour images. The methodology is based on an R-ordering (using the distance to a reference colour) completed by a C-ordering (using a lexicographical cascade). This framework could also be valid to develop other rank-based operators such as colour median filters.

The effects of these operators have been illustrated by means of different examples: colour image simplification using levelings, colour feature extraction using openings (closings) by reconstruction, colour gradients for segmenting, colour denoising by the centre operator, colour enhancement by the contrast mapping, etc. We have shown the suitability of the approach with examples from natural colour images and biomedical microscopic colour images. Exhaustive tests to evaluate quantitatively the performance of different orderings for the corresponding image processing tasks can be the object of future studies. Nevertheless, we hope that we have succeeded in giving the reader an impression of the potential of this approach.

The results of this paper have to be considered as a first step towards a general methodology of multivariate morphology using total ordering based on distance to references completed with a cascade of conditions. In future work we want to address various other important issues such as: the study of theoretical properties of operators derived from these orderings; the investigation of alternatives orderings based on other measures (correlations, projections, etc.) between the points and the reference, or based on a kind of fuzzification; the definition of particular orderings for other multivariate data such as hyper-spectral images, images of temporal series, etc.

References

[1] H. Al-Otum, Morphological operators for color image processing based on Mahalanobis distance measure, SPIE Optical Engineering Journal 42 (9) (2003) 2595–2606.

[2] J. Angulo, Morphologie mathématique et indexation d'images couleur. Application à la microscopie en biomédecine. Ph.D. Thesis, Ecole des Mines, Paris, December 2003.

[3] J. Angulo, J. Serra, Automatic analysis of DNA microarray images using mathematical morphology, Bioinformatics 19 (5) (2003) 553–562.

[4] J. Angulo, J. Serra, Morphological coding of color images by vector connected filters, in: Proceedings of IEEE 7th International Symposium on Signal Processing and Its Applications (ISSPA'03), Paris, July 2003, vol. I, pp. 69–72.

[5] J. Angulo, Unified morphological color processing framework in a lum/sat/hue representation, in: Proceedings of International Symposium on Mathematical Morphology (ISMM'05), Kluwer, 2005, pp. 387–396.

[6] J. Angulo, J. Serra, Modelling and segmentation of colour images in polar representations, Image and Vision Computing 25 (4) (2007) 475–495.

[7] J. Astola, P. Haavisto, Y. Nuevo, Vector median filters, Proceedings of the IEEE 78 (4) (1990) 678–689.

[8] V. Barnett, The ordering of multivariate data, Journal Of The Royal Statistical Society A 139 (3) (1976) 318–354.

[9] S. Beucher, F. Meyer, The morphological approach to segmentation: the watershed transformation, in: E. Dougherty (Ed.), Mathematical Morphology in Image Processing, Marcel-Dekker, New York, 1992, pp. 433–481.

[10] T. Boenisch (Ed.), Immunochemical Staining Methods Handbook, third ed., DakoCytomation, Carpinteria, CA, USA, 2001.

[11] P.O. Brown, D. Botstein, Exploring the NewWorld of the genome with DNA microarrays, Nature Genetics 21 (Suppl.) (1999) 33–37.

[12] C. Busch, M. Eberle, Morphological operations for color-coded images, in: EUROGRAPHICS '95, Computer Graphics Forum, vol. 14 (3), 1995, pp. C193–C204.

[13] T. Carron, P. Lambert, Color edege detector using jointly Hue, Saturation and Intensity, in: Proceedings of IEEE International Conference on Image Processing (ICIP'94), 1994, pp. 977–981.

[14] J. Chanussot, P. Lambert, Total ordering based on space filling curves for multivalued morphology, in: H.J.A.M. Heijmans, J.B.T.M. Roerdink (Eds.), Mathematical Morphology and its Applications to Image and Signal Processing (Proceedings of ISMM'98), Kluwer, 1998, pp. 51–58.

[15] M.L. Comer, E.J. Delp, Morphological operations for colour image processing, Journal of Electronic Imaging 8 (3) (1999) 279–289.

[16] S. Gibson, J.A. Bangham, R. Harvey, Evaluating a colour morphological scale-space, in: Proceedings of British Machine Vision Conference (BMVC'03), Norwich UK, July 2003.

[17] J. Goutsias, H.J.A.M. Heijmans, K. Sivakumar, Morphological operators for image sequences, Computer Vision and Image Understanding 62 (3) (1995) 326–346.

[18] A. Hanbury, J. Serra, Mathematical morphology in the HLS colour space, in: Proceedings 12th British Machine Vision Conference (BMV'01), Manchester, 2001, pp. II-451–460.

[19] A. Hanbury, J. Serra, Morphological operators on the unit circle, IEEE Transactions on Image Processing 10 (12) (2001) 1842–1850.

[20] A. Hanbury, J. Serra, Mathematical morphology in the CIELAB space, Image Analysis and Stereology 21 (3) (2002) 201–206.

[21] H.J.A.M. Heijmans, Morphological Image Operators, Academic Press, Boston, 1994.

[22] H.J.A.M. Heijmans, R. Keshet, Inf-semilattice approach to self-dual morphology, Journal of Mathematical Imaging and Vision 17 (1) (2002) 55–80.

[23] M. Iwanowski, J. Serra, Morphological interpolation and color images, in: Proceedings of ICIAP'99, Venice, Italy, 1999.

[24] G.M. Johnson, M.D. Fairchild, Visual Psychophysics and Color Appearance, in: CRC Digital Color Imaging Handbook, 2003.

[25] M. Köppen, Ch. Nowack, G. Rösel, Fuzzy-subsethood based color image processing, in: Proceedings of the 11th Scandinavian Conference on Image Analysis (SCIA'99), Kangerlussnaq, Greenland, vol. 1, 1999, pp. 195–202.

[26] H. Kramer, J. Bruckner, Iterations of non-linear transformations for enhancement on digital images, Pattern Recognition 7 (1975) 53–58.

[27] J. Li, Y. Li, Multivariate mathematical morphology based on principal component analysis: initial results in building extraction, in: Proceedings of the 20th ISPRS Congress, Instanbul, Turkey, vol. 35(B7), 2004, pp. 1168–1173.

[28] G. Louverdis, M.I. Vardavoulia, I. Andradis, Ph. Tsalides, A new approach to morphological color image processing, Pattern Recognition 35 (2002) 1733–1741.

[29] R. Lukac, K.N. Plataniotis, B. Smolka, A.N. Venetsanopoulos, A multichannel order-statistic technique for cDNA microarray image processing, IEEE Transactions on Nanobioscience 3 (4) (2004) 272–285.

[30] R. Lukac, K.N. Plataniotis, B. Smolka, A.N. Venetsanopoulos, cDNA microarray image processing using fuzzy vector filtering framework, Journal of Fuzzy Sets and Systems 152 (1) (2005) 17–35.

[31] R. Lukac, B. Smolka, K. Martin, K.N. Plataniotis, A.N. Venetsanopoulos, Vector filtering for color imaging, IEEE Signal Processing Magazine 22 (1) (2005) 74–86.

[32] R. Lukac, K.N. Plataniotis, A taxonomy of color image filtering and enhancement solutions, in: P.W. Hawkes (Ed.), Advances in Imaging and Electron Physics, vol. 140, Elsevier, 2006, pp. 187–264.

[33] F. Meyer, J. Serra, Contrasts and activity lattice, Signal Processing 16 (1989) 303–317.

[34] F. Meyer, The levelings, in: H.J.A.M. Heijmans, J.B.T.M. Roerdink (Eds.), Mathematical Morphology and its Applications to Image and Signal Processing (Proceedings of ISMM'98), Kluwer, 1998, pp. 199–206.

[35] A. Mojsilovic, E. Soljanin, Quantization of color spaces and processing of color images by fibonacci lattices, in: Proceedings of Human Vision and Electronic Imaging V, vol. SPIE 3959, 2000, pp. 345–355.

[36] F. Ortiz, F. Torres, P. Gil, J. Pomares, S. Puente, F. Candelas, Vectorial ordering by distance for HSI mathematical morphology, in: Proceedings of the IX Spanish Symposium on Pattern Recognition and Image Analysis, Castellón, Spain, vol II, 2001, pp. 379–384.

[37] F. Ortiz, F. Torres, J. Angulo, S. Puente, Comparative study of vectorial morphological operations in different color spaces, in: Proceedings of the SPIE Conference on Intelligent Robots and Computer Vision XX, Boston, MA, SPIE vol. 4572, November 2001, pp. 259–268.

[38] S. Osher, L.I. Rudin, Feature-oriented image enhancement using shock filters, SIAM Journal of Numerical Analysis 27 (1990) 919–940.

[39] R.A. Petters II, Mathematical morphology for angle-valued images, in: Proceedings of Non-Linear Image Processing VIII, vol. SPIE 3026, 1997, pp. 84–94.

[40] I. Pitas, P. Tsakalides, Multivariate ordering in color image processing, IEEE Transactions on Circuits Systems Video Technology 1 (3) (1991) 247–256.

[41] A. Plaza, P. Martinez, R. Perez, J. Plaza, Spatial/spectral endmember extraction by multidimensional morphological operations, IEEE Transactions on Geoscience and Remote Sensing 40 (9) (2002) 2025–2041.

[42] Ch. Ronse, V. Agnus, Morphology on label images: flat-type operators and connections, Journal of Mathematical Imaging and Vision 22 (2005) 283–307.

[43] L.J. Sartor, A.R. Weeks, Morphological operations on color images, Electronic imaging 10 (2) (2001) 548–559.

[44] J. Serra, Image analysis and mathematical morphology. Vol I, and Image Analysis and Mathematical Morphology. Vol II: Theoretical Advances, Academic Press, London, 1982, 1988.

[45] J. Serra, Toggle mappings, in: J.C. Simon (Ed.), From Pixels to Features, Amsterdam, North Holland, 1989, pp. 61–72.

[46] J. Serra, Anamorphoses and function lattices (multivalued morphology), in: E.R. Dougherty (Ed.), Mathematical Morphology in Image Processing, Marcel-Dekker, 1992, pp. 483–523.

[47] J. Serra, Espaces couleur et traitement d'images, CMM-Ecole des Mines de Paris, Internal Note N-34/02/MM, October 2002, 13 p.

[48] J. Serra, Morphological segmentation of colour images by merging of partitions, in: Proceedings of International Symposium on Mathematical Morphology (ISMM '05), Kluwer, 2005, pp. 151–176.

[49] J. Slavik (Ed.), Fluorescence Microscopy and Fluorescent Probes, vol. 2, Plenum Press, New York, USA, 1998, 423 p.

[50] H. Talbot, C. Evans, R. Jones, Complete ordering and multivariate mathematical morphology: algorithms and applications, in: Proceed-

ings of the International Symposium on Mathematical Morphology (ISMM'98), Kluwer, pp. 27–34.

[51] P.E. Trahanias, D. Karakos, A.N. Venetsanopoulos, Directional processing of color images: theory and experimental results, IEEE Transactions on Image Processing 5 (6) (1996) 868–880.

[52] M.I. Vardavoulia, I. Andreadis, Ph. Tsalides, A new vector median filter for colour image processing, Pattern Recognition Letters 22 (6–7) (2001) 675–689.

[53] L. Vincent, Morphological grayscale reconstruction in image analysis: applications and efficient algorithms, IEEE Transactions on Image Processing 2 (2) (1993) 176–201.

[54] K.R. Weber, S.T. Acton, On connected filters in color image processing, Journal of Electronic Imaging 13 (3) (2004) 619–629.

[55] A.R. Weeks, L.J. Sartor, Color morphological operators using conditional and reduced ordering, in: Proceedings of the SPIE Conference on Applications of Digital Image Processing XXII, vol. SPIE 3808, 1999, pp. 358–366.

[56] M. Wheeler, Z.A. Zmuda, Processing color and complex data using mathematical morphology, in: Proceedings of the IEEE National Aerospace and Electronics Conference (NAECON 2000), 2000, pp. 618–624.

[57] S.S. Wilson, Theory of matrix morphology, IEEE Transaction on Pattern Analysis and Machine Intelligence 14 (1992) 636–652.

[58] G. Wyszecki, W.S. Stiles, Color Science: Concepts and Methods, Quantitative Data and Formulae, second ed., John Wiley & Sons, New-York, 1982.

[59] E. Zaharescu, M. Zamfir, C. Vertan, Color morphology-like operators based on color geometric shape characteristics, in: Proceedings of International Symposium on Signals, Circuits and Systems (SCS'03), vol. 1, 2003, pp. 145–148.